

LoopServe: An Adaptive Dual-phase LLM Inference Acceleration System for Multi-Turn Dialogues

Haoyang LI
Computing, PolyU
haoy1li@comp.polyu.edu.hk

Zhanchao XU
Computing, PolyU
zhanchaoxu0228@gmail.com

Yiming LI
Noah’s Ark Lab, Huawei
li.yiming3@huawei.com

Xuejia CHEN
Computing, PolyU
gresham15437@gmail.com

Darian LI
Computing, PolyU
jinlulhc@outlook.com

Anxin TIAN
EMIA, HKUST
atian@connect.ust.hk

Qingfa XIAO
DSA, HKUST(GZ)
qxiao183@connect.hkust-
gz.edu.cn

Cheng DENG
Bayes Centre & CSE, Edin
davendw49@gmail.com

Jun WANG
AI Centre & CS, UCL
jun.wang@cs.ucl.ac.uk

Qing LI
Computing, PolyU
csqli@comp.polyu.edu.hk

Lei CHEN
DSA, HKUST(GZ)
leichen@cse.ust.hk

Mingxuan YUAN
Noah’s Ark Lab, Huawei
yuan.mingxuan@huawei.com

Abstract

Multi-turn dialogues are essential in many real-world applications of large language models, such as chatbots and virtual assistants. As conversation histories become longer, existing large language models face increasing computational and memory challenges, which hinder their ability to provide efficient and responsive interactions. Most current acceleration methods either compress the context or optimize key value caching, but they often rely on fixed or position-based heuristics that do not adapt well to the dynamic and unpredictable patterns found in actual multi-turn conversations. In this paper, we present LoopServe, an adaptive dual-phase inference acceleration framework for large language models in multi-turn dialogues. LoopServe introduces two main innovations. First, it performs online sparsification during the prefilling phase by dynamically selecting the most important parts of the attention matrix for each new input. Second, it uses progressive key value compression during decoding by adaptively maintaining a relevant and efficient cache based on the most recently generated output tokens. We also propose a new benchmark with eleven multi-turn datasets that reflect realistic query positions and conversational dependencies. Extensive experiments demonstrate that LoopServe consistently achieves superior effectiveness compared to existing baselines and significantly accelerates LLM inference across a wide range of long-context dialogue tasks.

PVLDB Reference Format:

Haoyang LI, Zhanchao XU, Yiming LI, Xuejia CHEN, Darian LI, Anxin TIAN, Qingfa XIAO, Cheng DENG, Jun WANG, Qing LI, Lei CHEN, and Mingxuan YUAN. LoopServe: An Adaptive Dual-phase LLM Inference Acceleration System for Multi-Turn Dialogues. PVLDB, 18(1): XXX-XXX, 2025. doi:XX.XX/XXX.XX

This work is licensed under the Creative Commons BY-NC-ND 4.0 International License. Visit <https://creativecommons.org/licenses/by-nc-nd/4.0/> to view a copy of this license. For any use beyond those covered by this license, obtain permission by emailing info@vldb.org. Copyright is held by the owner/author(s). Publication rights licensed to the VLDB Endowment.

Proceedings of the VLDB Endowment, Vol. 18, No. 1 ISSN 2150-8097.
doi:XX.XX/XXX.XX

1 Introduction

Multi-turn dialogues are at the core of numerous real-world applications, from customer service chatbots to virtual assistants and collaborative agents. These scenarios demand that large language models (LLMs) [14, 22, 37, 58, 74] not only generate coherent responses but also maintain contextual consistency across lengthy, evolving conversations. As the number of dialogue turns increases, so does the computational workload. For instance, processing a multi-turn dialogue comprising 10,000 tokens with Llama-3.1-70B [21] can demand trillions of floating-point operations (FLOPs), quickly challenging the limits of real-time inference. Despite the remarkable progress of LLMs such as GPT [7, 49, 50], Llama [21, 57], and DeepSeek [12, 13], their inefficiency in handling multi-turn dialogues remains largely unaddressed.

In a typical multi-turn setting, each new user turn expands the conversation history, requiring the LLM to process ever-growing input sequences. The model’s self-attention mechanism, which lies at the heart of the Transformer [59], needs to compute pairwise attention scores between every pair of tokens in the input. Specifically, given an input sequence of length n , an LLM with P parameters and a hidden dimension d , the time complexity of generating m tokens is $O(m((n+m)^2d + P))$. For instance, in a 3-turn conversation with 5000 tokens per turn, the effective context length for the model reaches 15,000 tokens, resulting in quadratic growth in both computational cost and memory usage. This compounding effect of context accumulation makes real-time, cost-efficient inference increasingly difficult as the conversation progresses.

This challenge is distinct from single-turn tasks, where the input context is static and the user query is typically placed at the end of the sequence. In contrast, multi-turn dialogues feature dynamic context accumulation and variable query positions: user questions may appear at the beginning, middle, or end of the input. This variability causes the attention patterns within the model to change unpredictably across turns and inputs, requiring the model to flexibly maintain and retrieve relevant information from any point in the conversation. The resulting attention matrices not only grow

in size with each turn but also exhibit highly dynamic and input-dependent sparsity patterns, further exacerbating the inefficiency of existing inference methods.

Recent research on LLM inference acceleration has primarily focused on two directions: context compression and Key-Value (KV) compression. Firstly, Context compression techniques, such as LLMingua [47], CompAct [66], and RAG-based approaches [9, 15, 30, 60, 60, 72], reduce input length by filtering, summarizing, or structuring the context. While effective in lowering computational costs, these strategies often sacrifice fine-grained details, which can degrade output fidelity. Secondly, KV compression approaches aim to reduce the computational burden of attention weight calculations during both the prefilling and decoding stages. In the prefilling stage, where the attention matrix is computed for all token pairs, methods [28, 32, 43], such as Minference [28], sparsify the attention matrix to reduce quadratic computation (See Table 2). In the decoding stage, KV caches store precomputed Key and Value vectors for reuse, minimizing redundant computations during autoregressive text generation. For example, H2O [71], PQCache [68], SnapKV [39], and AdaKV [18] select or cache only the most relevant tokens based on attention weights or fixed token positions. However, these methods predominantly rely on static or position-based heuristics, which are ill-suited for the dynamic, input-dependent patterns observed in real-world multi-turn dialogues.

Moreover, current evaluation benchmarks [2, 24, 31, 36, 37] for LLM acceleration misrepresent real-world dialogue scenarios. Most benchmarks [5, 10, 36] assume queries are always placed at the end of the input and focus on single-turn tasks, which oversimplifies the problem and favors acceleration methods that exploit positional biases. As a result, approaches [18, 39, 71] that perform well on these benchmarks often fail to generalize to realistic dialogue scenarios where queries may appear at arbitrary positions and contextual dependencies span multiple turns.

To address these challenges, we conduct experiments and summarize three key findings: (1) The sparsity patterns of attention matrices are highly dynamic across inputs, heads, and layers. A small fraction of vertical and slash lines in the attention matrix accounts for most attention weights, but these patterns vary significantly and cannot be effectively captured by static or offline sparsification methods. (2) The position of questions in user queries significantly affects the performance of existing LLM acceleration techniques, which assume queries are always at the end of the input sequence. However, queries often appear in the middle or beginning of the context. (3) Token importance evolves dynamically during multi-turn dialogues as new outputs are generated. Fixed token selection strategies fail to capture these changing dependencies, leading to inefficiencies and reduced conversational quality.

Based on these observations, we propose LoopServe, an adaptive dual-phase LLM inference acceleration framework specifically designed for multi-turn dialogues. LoopServe introduces two key innovations: online prefilling sparsification and progressive KV compression. In the prefilling phase, LoopServe dynamically identifies and selects the most critical components of the attention matrix, specifically the vertical and slash lines that account for the majority of attention weights. Unlike fixed sparsification methods, LoopServe adapts online, ensuring computational efficiency while maintaining high attention fidelity. In the decoding phase,

LoopServe employs a progressive KV compression strategy. It dynamically selects and compresses relevant input tokens based on the most recently generated output tokens. This approach ensures the KV cache remains efficient and relevant throughout the decoding process, significantly reducing computational overhead without compromising output quality. Also, we propose a multi-turn long-context benchmark, including 11 datasets. This benchmark captures diverse query positions and multi-turn dependencies, providing a more realistic evaluation framework for multi-turn dialogue scenarios. The contributions of this paper are summarized as follows:

- We empirically demonstrate that attention patterns and key token positions in multi-turn dialogues are highly dynamic and unpredictable, revealing the limitations of static sparsification and KV selection methods.
- We introduce LoopServe, a novel dual-phase LLM inference acceleration system that integrates online attention sparsification and progressive KV compression, substantially improving efficiency and robustness for multi-turn dialogue inference.
- We propose a new benchmark with 11 diverse multi-turn datasets. This benchmark incorporates diverse query positions and multi-turn dependencies, offering a comprehensive evaluation framework for LLMs in realistic long-context conversational tasks.
- Extensive experiments conducted on 11 long-context multi-turn datasets demonstrate that LoopServe consistently outperforms state-of-the-art LLM acceleration models.

2 Preliminary and Related Work

In this section, we first introduce the preliminary of LLMs in Section 2.1, and then introduce various techniques that enhance the efficiency of long-context LLM inference in Section 2.2. Finally, we analyze existing benchmarks for LLM acceleration in Section 2.3.

2.1 Large Language Models

LLMs, such as GPT [7], Llama [21], and DeepSeek [12, 13], demonstrate exceptional abilities in context understanding and reasoning, achieving significant success in various tasks, such as data cleaning [3, 16, 19, 45, 52, 54, 64, 77], data management [23, 26, 33, 35, 41, 44, 55, 69], data visualization [4, 61], data security [38], recommendation system [65, 73], text to SQL [17, 34, 42, 51, 58, 70, 75], and information extraction [8, 11, 25, 27, 46, 53, 55, 63, 67, 76]. Their impressive performance stems from extensive training datasets and a transformer architecture, which effectively captures long-range dependencies and enables advanced autoregressive generation.

2.1.1 Transformer Decoder The effectiveness of Transformer decoders stems from the Multi-Head Self-Attention (MHSA) mechanism, which efficiently captures both local and global dependencies among input tokens. For clarity, we analyze a single representative Transformer block, as the operational principles are consistent across all blocks in the architecture. Given an input token sequence $X = [x_1, x_2, \dots, x_n]$ with embeddings $\mathbf{X} \in \mathbb{R}^{n \times d}$, the self-attention mechanism computes weighted aggregations over the token sequence, where the weights are derived from inter-token similarity scores. Specifically, the MHSA mechanism generates query vectors $\mathbf{Q}^i \in \mathbb{R}^{n \times d_k}$, key vectors $\mathbf{K}^i \in \mathbb{R}^{n \times d_k}$, and value vectors $\mathbf{V}^i \in \mathbb{R}^{n \times d_v}$

for the i -th attention head through learned linear transformations:

$$\mathbf{Q}^i = \mathbf{X}\mathbf{W}_{Q^i}, \quad \mathbf{K}^i = \mathbf{X}\mathbf{W}_{K^i}, \quad \mathbf{V}^i = \mathbf{X}\mathbf{W}_{V^i}, \quad (1)$$

where $\mathbf{W}_{Q^i} \in \mathbb{R}^{d_x \times d_k}$, $\mathbf{W}_{K^i} \in \mathbb{R}^{d_x \times d_k}$ and $\mathbf{W}_{V^i} \in \mathbb{R}^{d_x \times d_v}$ are learnable parameters. The self-attention operation is subsequently applied to each triple $(\mathbf{Q}^i, \mathbf{K}^i, \mathbf{V}^i)$, yielding the output of the i -th attention head \mathbf{Z}^i as follows:

$$\mathbf{Z}^i = \text{Attention}(\mathbf{Q}^i, \mathbf{K}^i, \mathbf{V}^i) = \text{Softmax}\left(\frac{\mathbf{Q}^i(\mathbf{K}^i)^\top}{\sqrt{d_k}}\right)\mathbf{V}^i, \quad (2)$$

where the scaling factor $\sqrt{d_k}$ ensures numerical stability [59]. To capture diverse semantic relationships, h parallel attention heads process \mathbf{X} concurrently. Then, $\mathbf{Z} = \text{Concat}(\mathbf{Z}^1, \mathbf{Z}^2, \dots, \mathbf{Z}^h)\mathbf{W}_O$, where Concat is the concatenation operation, and $\mathbf{W}_O \in \mathbb{R}^{h \cdot d_v \times d_o}$ is the trainable projection matrix. Following the self-attention mechanism, the output is passed through a Feed Forward Network, whose result serves as the input to the next Transformer block.

2.1.2 Auto-regressive Generation Mechanism LLMs utilize an autoregressive generation paradigm, where text is produced sequentially with each token conditioned on the tokens generated before it. This step-by-step approach maintains semantic coherence and ensures contextual relevance across the output. Formally, given an input sequence $X = [x_1, x_2, \dots, x_n]$, LLM predicts the subsequent token x_{n+1} by estimating the conditional probability distribution:

$$P(x_{n+1}|x_1, x_2, \dots, x_n) = \text{Softmax}(\mathbf{h}_n \mathbf{W}_{\text{out}} + \mathbf{b}_{\text{out}}), \quad (3)$$

where $\mathbf{h}_n \in \mathbb{R}^{d_h}$ represents the hidden state encoding for sequence X at step n , $\mathbf{W}_{\text{out}} \in \mathbb{R}^{d_h \times n_{\text{vocal}}}$ denotes the output projection matrix mapping to vocabulary size n_{vocal} . The softmax function transforms logits into a probability distribution across the vocabulary space. During generation, the model samples the next token x_{n+1} from the computed probability distribution: $x_{n+1} \sim P(x_{n+1}|x_1, x_2, \dots, x_n)$. The newly generated token x_{n+1} is appended to the sequence X to obtain resulting $X = [x_1, \dots, x_n, x_{n+1}]$. This process iterates until either a designated end-of-sequence (EOS) token is produced or a predetermined maximum sequence length is reached.

2.2 Efficient Long-Context Inference

The impressive abilities of LLMs across various tasks weaken significantly when handling long contexts. This happens mainly because of basic limits in computation and memory. The drop in performance, especially efficiency, is due to the quadratic complexity of self-attention mechanisms in Equation (2), which require calculating interactions between every pair of tokens in the input sequence. Specifically, for an LLM architecture comprising L layers with h attention heads per layer, processing an input sequence of length n requires computational operations scaling at $O(Lhn^2)$. This quadratic growth in both computational demand and memory utilization renders the handling of extensive sequences prohibitively expensive [37]. To overcome these efficiency challenges, researchers have created specialized techniques to speed up long-context LLM processing. These methods typically fall into two main categories: context compression and KV-based optimization.

Table 1: Summary of important notations.

Symbol	Definition
X_i	Input sequence of tokens
$X_{i,j}$	The j -turn input of X_i
Y_i	Output sequence of tokens
$y_{i,j}$	The j -turn output of X_i
$n_i, n_{i,j}$	Length of input sequence X_i and $X_{i,j}$
$m_i, m_{i,j}$	Length of output sequence Y_i and $y_{i,j}$
M_θ	LLM model
n_h	The total number of attention head of M_θ
$\mathbf{Q}_i^k, \mathbf{K}_i^k, \mathbf{V}_i^k$	Query, Key, and Value matrices
\mathbf{A}_i^k	The k -th attention head X_i
$\mathcal{S}_i^k, \mathcal{V}_i^k$	Slash and vertical lines of head \mathbf{A}_i^k
$\hat{\mathcal{S}}_i^k, \hat{\mathcal{V}}_i^k$	Selected slash lines and vertical lines
n_d	Decoding interval
B	Budget for input tokens
\hat{X}_i^k	Selected important tokens for attention head k

2.2.1 Context Compression Methods Context compression strategies aim to reduce effective sequence length by systematically eliminating non-essential content or distilling key information from verbose inputs. These approaches effectively transform lengthy inputs into more computationally manageable representations. Firstly, the filtering-based methods, such as LLMingua [29], LLMingua-v2 [47], and CompAct [66], selectively identify and preserve high-relevance content, enabling models to process critical information without engaging the entire sequence at maximum resolution. Alternatively, RAG-based techniques [9, 15, 30, 60, 72] employ a two-stage process: initially constructing knowledge graphs through extraction of essential semantic triples from input text, followed by synthesizing this structured knowledge into condensed representations that serve as reduced-dimension inputs for LLM processing. While these compression strategies substantially reduce computational and memory requirements during inference, they inevitably sacrifice some degree of granular detail, potentially compromising the fidelity and precision of LLM-generated outputs.

2.2.2 KV-based Optimization To mitigate the computational burden, KV-based approaches focus on reducing the number of attention weight calculations during both prefilling and decoding stages, as summarized in Table 2.

Prefilling-stage Optimization. Given an input X_i with n_i length, the prefilling stage requires $O(n_i^2)$ computations to compute each attention matrix across all token pairs, which is a significant computational bottleneck. Recent approaches such as Minference [28], FlexPrefill [32], and CritiPrefill [43] address this by selectively discarding negligible attention values, effectively sparsifying each attention head matrix:

$$\min \left| \mathbf{A}_i^j - \hat{\mathbf{A}}_i^j \right|, \text{ s.t. }, \hat{\mathbf{A}}_i^j = \text{Softmax}\left(\frac{\mathbf{Q}^j(\mathbf{K}^j)^\top}{\sqrt{d_k}} - c(1 - \mathbf{M})\right),$$

where $\mathbf{M} \in \{0, 1\}^{n \times n}$ represents a binary sparsity mask, where $\mathbf{M}[a][b] = 1$ indicates that the attention weight $\mathbf{A}_i^j[a][b]$ should be preserved. The constant $c = 10^8$ ensures that masked positions ($\mathbf{M}[a][b] = 0$) receive negligible attention weight after softmax

normalization. This optimization reduces the computational complexity from $O(n^2)$ to $O(\alpha n^2)$ per head, where the sparsity factor $\alpha \ll 1$. Specifically, Minference [28] improves efficiency by selecting key vertical and slash attention patterns or important blocks, while FlexPrefill [32] enhances this approach by dynamically adjusting the sparsity rate based on attention recovery rates. In contrast, CritiPrefill [43] partitions keys and queries into blocks and simply selects the top- k most important key blocks for computation. However, as shown by our motivational experiments (Section 3), the sparsity and importance patterns in attention matrices are highly dynamic and input-dependent, varying significantly across turns, heads, and layers. Consequently, fixed-pattern selection approaches often fail to achieve robust performance in real multi-turn scenarios.

Decoding-stage Optimization. During autoregressive text generation, LLMs utilize KV caches to store and reuse partial previously computed Key and Value embeddings, thereby reducing computational redundancy. Firstly, token-level selection approaches [20, 39], such as H2O [71], SnapKV [39], and AdaKV [18], aim to select important tokens from inputs before output generation. These methods assume that critical input tokens required for generating outputs can be identified beforehand and that these tokens significantly overlap with those in the last observation window of the inputs. As analyzed in Section 3, these approaches perform well on existing benchmarks like LongBench [5, 6], because such benchmarks place user queries at the end of the input sequence. This assumption holds in existing benchmarks, where user queries are always placed at the end of the input sequence. In such settings, token-level selection methods perform well: by focusing on the most recent tokens (which include the user query), these methods can accurately preserve the necessary context for high-quality output, while significantly reducing memory and computation.

However, this benchmark design does not match real-world multi-turn dialogues, where user queries can appear anywhere in the input. When queries are not always at the end, token-level selection methods like SnapKV [39] and AdaKV [18] often miss the critical tokens needed for accurate output, resulting in lower performance and poor generalization. As shown in Section 3.2, their effectiveness drops significantly when queries are in the middle or at the front of the context. This highlights the need for adaptive, context-aware KV selection methods that can handle dynamic query positions and dependencies in practical dialogue scenarios.

2.3 Long-Context Benchmarks

Recently, various long-context benchmarks [2, 24, 31, 36, 37, 48] have been proposed to evaluate LLMs, such as NumericBench [36], LongBench [5, 6], and LongEval [10]. However, these benchmarks have two significant limitations that hinder their applicability to real-world scenarios. First, they assume that user queries are always positioned at the end of the input context. This architectural bias simplifies the evaluation process but fails to capture the complexity of real-world interactions, where queries may appear at the beginning, middle, or interspersed throughout the input. As a result, existing KV-compression approaches perform well on these benchmarks because they are optimized for scenarios where the user question is placed at the end of the input. However, these methods struggle to generalize to real-world human-LLM interactions.

Table 2: LLM acceleration model comparisons, following [40]. P and D denote whether the model has optimization in the Prefilling and Decoding phases, respectively. n is the token size of the input, m is the generation token size, and c and k are constants with $c, k \ll n$ and $c, k \ll m$.

Methods	P	D	KV Size Prefilling	Decoding	
LLMLingua [47]	✓	×	$O(\alpha n)$	$O(\alpha^2 n^2)$	$O(\alpha n m)$
A-shape [62]	✓	×	$O(n)$	$O(kn)$	$O(nm)$
Tri-shape [40]	✓	×	$O(n)$	$O(kn)$	$O(nm)$
Minference [28]	✓	×	$O(n)$	$O(kn)$	$O(nm)$
SLLM [62]	×	✓	$O(k)$	$O(n^2)$	$O(km)$
SnapKV [39]	×	✓	$O(k)$	$O(n^2)$	$O(km)$
AdaKV [18]	×	✓	$O(k)$	$O(n^2)$	$O(km)$
LoopServe	✓	✓	$O(k)$	$O(kn)$	$O(k(m-c) + nc)$

Second, most of these benchmarks are single-turn, focusing on isolated question-answering or summarization tasks. This approach overlooks the multi-turn nature of real-world conversations, where contextual dependencies across multiple turns are critical [40].

To address these limitations, we propose a multi-turn benchmark with 11 datasets in Section 4 with diverse query positions and interaction patterns, providing a more realistic evaluation of LLMs for long-context tasks.

3 Motivational Experiments and Insights

To better understand the fundamental challenges of accelerating LLM inference in multi-turn dialogues, we conduct a series of motivational experiments. These experiments, presented in Sections 3.1 and 3.2, provide key observations on the dynamic sparsity of attention patterns and the impact of query position on acceleration effectiveness. Based on these insights, we introduce the LoopServe system in Section 5, which is specifically designed to address these unique challenges in real-world multi-turn dialogue scenarios.

3.1 Key Point 1: Uncertain Attention Patterns

As discussed in Section 2, each attention head matrix is highly sparse. Current approaches [18, 28, 39, 40, 62] for accelerating the prefilling and decoding phases often rely on attention matrix sparsification and important KV token selection. However, these methods are built on a strong assumption: the attention sparsification during the prefilling and important tokens in decoding follow fixed patterns, and their positions can be identified offline. However, the sparsity patterns of attention matrices are dynamic and unpredictable, varying across different inputs, heads, and layers. This variability challenges the effectiveness of fixed-pattern approaches. In this subsection, we first reveal the sparsity of each attention head and then demonstrate that the sparsity patterns vary across different attention heads and input sequences.

3.1.1 Motivational Observation 1: only 90% of vertical lines and slash lines can collectively account for most (e.g., 90%) of the attention weight. In the attention matrix, a vertical line is a single column, showing that one token is attended to by all other tokens in the sequence. This often happens with special tokens like separators or keywords. A slash line is a diagonal, showing that each

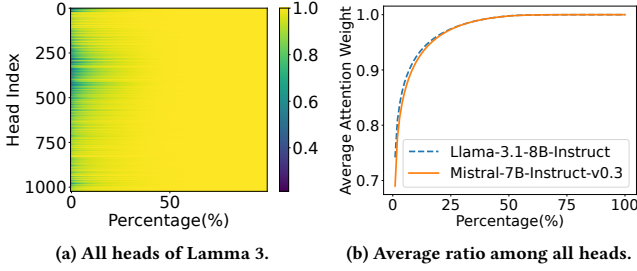


Figure 1: Attention head sparsity. Only a small fraction of vertical and slash lines in each attention head of LLMs can recover most of the attention weights, revealing strong sparsity in the attention matrix.

token mainly focuses on its nearby tokens, which is a pattern of local attention. We conduct experiments on a SAMSum QA [5] dataset $\mathcal{D} = \{(X_i, Y_i)\}_{i=1}^{|\mathcal{D}|}$ using the Llama-3.1-8B-Instruct model with n_h attention heads. For each user query X_i of length n_i , each k -th attention matrix $A_i^k \in \mathbb{R}^{n_i \times n_i}$ contains n_i slash lines S_i^k and n_i vertical lines \mathcal{V}_i^k . The total attention weight for each slash line $s^k \in S_i^k$ is computed as $\sum_{(a,b) \in s^k} A_i^k[a][b]$, and the total attention weight for each vertical line $v^k \in \mathcal{V}_i^k$ is $\sum_{(a,b) \in v^k} A_i^k[a][b]$. Next, we only use the top $\eta \cdot 2n_i$ slash lines $\hat{S}_i^k \subseteq S_i^k$ and vertical lines $\hat{\mathcal{V}}_i^k \subseteq \mathcal{V}_i^k$. Therefore, for each k -th attention head, the ratio of the attention weight within these selected lines to the total attention weight can

be computed as follows: $r_i^k = \frac{1}{|\mathcal{D}|} \sum_{X_i \in \mathcal{D}} \frac{\sum_{(a,b) \in \hat{S}_i^k \cup \hat{\mathcal{V}}_i^k} A_i^k[a][b]}{n_i}$. Also, the average ratio among n_h attention heads can be computed as $\frac{1}{n_h} \sum_{j=1}^{n_h} r_j^k$. As shown in Figure 1 (a), increasing η raises the accumulated attention weight across different heads; a small percentage of slash and vertical lines captures most of the attention weight. Figure 1 (b) shows that both LLaMA and Mistral exhibit this sparsity: covering 90% of the total attention weight requires selecting only 10% of slash and vertical lines. This indicates that, due to the sparsity in attention heads, vertical and slash lines are fundamental for efficient selection.

3.1.2 Motivational Observation 2: The positions of the top vertical and slash lines within the same head vary across different user inputs. Given the LLM model M_θ with n_h attention heads, the dataset $\mathcal{D} = \{X_i\}_{i=1}^{|\mathcal{D}|}$, and the percentage η , we select the top- $\eta \cdot 2n_i$ slash lines $\hat{S}_i^k \subseteq S_i^k$ and vertical lines $\hat{\mathcal{V}}_i^k \subseteq \mathcal{V}_i^k$ for each user query X_i under each k -th head. For two queries X_i and X_j , we compute the line overlap of the selected vertical and slash lines as: $r_{i,j}^k = \frac{|\hat{S}_i^k \cap \hat{S}_j^k| + |\hat{\mathcal{V}}_i^k \cap \hat{\mathcal{V}}_j^k|}{|\hat{S}_i^k \cup \hat{S}_j^k| + |\hat{\mathcal{V}}_i^k \cup \hat{\mathcal{V}}_j^k|}$. The average important line overlap ratio across n_h heads can then be computed as $\frac{1}{n_h |\mathcal{D}|^2} \sum_{k=1}^{n_h} \sum_{X_i, X_j \in \mathcal{D}} r_{i,j}^k$. In particular, we use SAMSum QA [5] dataset along with Llama-3.1-8B-Instruct and Mistral-7B-Instruct-v0.3, and vary $\eta \in \{0.1, 0.15, 0.2, 0.25, 0.3\}$. As shown in Figure 2, the overlap of important lines across both LLMs is mostly below 0.5 for different inputs in most heads. This shows that different texts produce distinct line patterns, even within the same attention head. Therefore, it is not practical to identify important lines offline and use them directly for online inference.

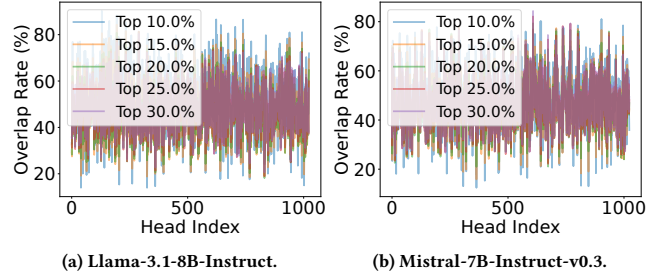


Figure 2: Line overlap of the same head with different inputs. The important attention lines differ significantly across inputs, even for the same attention head, highlighting the dynamic and input-dependent nature of attention sparsity.

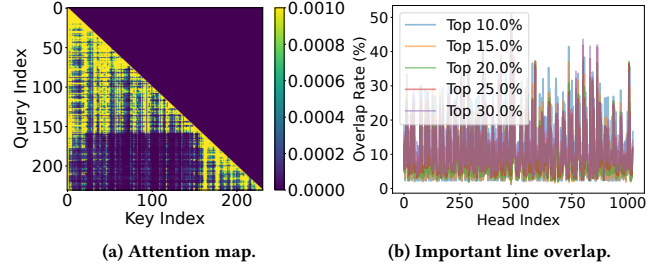


Figure 3: Different patterns in the same head. It illustrates that important attention lines differ even within different segments of the same input, emphasizing the locality and unpredictability of attention patterns.

3.1.3 Motivational Observation 3: Given an input $X_i = [C_i^1, C_i^2]$, where X_i consists of two sequential segments C_i^1 and C_i^2 . The important positions of the top vertical and slash lines within the same head differ between C_i^1 and C_i^2 . Both C_i^1 and C_i^2 exhibit their own local attention sparsity patterns. As shown in Figure 3 (a), the prominent slash and vertical lines in the attention matrix of C_i^1 do not appear in C_i^2 . Instead, the attention part of C_i^2 exhibits distinct local patterns. To qualitatively verify this, we use SAMSum QA [5] data with Llama-3.1-8B-Instruct to conduct experiments. Given the dataset $\mathcal{D} = \{X_i\}_{i=1}^{|\mathcal{D}|}$, each X_i is split into two sequential parts as $X_i = [C_i^1, C_i^2]$. We denote the attention matrix of C_i^1 as $A_{C_i^1}^k \in \mathbb{R}^{|C_i^1| \times |C_i^1|}$ and the attention matrix of C_i^2 as $A_{C_i^2}^k \in \mathbb{R}^{|C_i^2| \times n_i}$. Next, we select the top- η slash and vertical lines for $A_{C_i^1}^k$ and $A_{C_i^2}^k$, denoted as $L_{C_i^1}^k$ and $L_{C_i^2}^k$, respectively. The overlap rate of important lines between C_i^1 and C_i^2 as $r_{C_i^1 \rightarrow C_i^2}^k = \sum_{l \in L_{C_i^1}^k} \mathbb{I}(l \in L_{C_i^2}^k) / |L_{C_i^1}^k|$, where $\mathbb{I}(l \in L_{C_i^2}^k) = 1$ if the line $l \in L_{C_i^1}^k$, indicating that an important line l of C_i^1 is still important in C_i^2 . Then, given data \mathcal{D} and the k -th attention head, the average overlapping ratio is $\frac{1}{|\mathcal{D}|} \sum_{X_i \in \mathcal{D}} r_{C_i^1 \rightarrow C_i^2}^k$. As shown in Figure 3 (b), under different η , the overlap rate between contexts in a user query remains low and highly volatile, indicating distinct local attention patterns for different subsections of input X_i .

This observation directly highlights that it is challenging to use a subsection of the input to determine the patterns of the entire input, as distinct local patterns exist within different subsections.

Consequently, existing prefilling acceleration approaches, such as Minference [28], which rely on the last window (e.g., C_i^2) to determine the patterns for the whole input X_i and select important attention blocks, fail to achieve consistent performance in real-world applications. Similarly, decoding acceleration approaches, such as SnapKV [39], H2O [71], and Keyformer [1], which use the last observation window (e.g., last several tokens of C_i^1) to identify important tokens for generating outputs (e.g., the second context C_i^2), are also unreliable. As a result, these methods struggle to deliver good performance in practical scenarios.

3.2 Key Point 2: Question Position Matters.

Based on the above motivational experiments, both prefilling-based and decoding-phase acceleration approaches, that rely on offline sparse pattern discovery or fixed sparse patterns, should be incapable of performing well in real-world use cases. However, the results reported in their papers are often comparable to original LLMs using the full attention matrix without any compression. Why? The reason is that existing long-context benchmarks, such as Longbench [5, 6], place each user question q_i at the end of the input sequence $X_i = [C_i, q_i]$. Then, the LLMs will answer the question q_i based on the context C_i . In this setup, by relying only on the last observation window of the input (i.e., the user questions), existing acceleration approaches identify important tokens in the context that are highly correlated with the user’s specific questions. This partially alleviates the uncertainty caused by distinct local patterns observed in real-world scenarios.

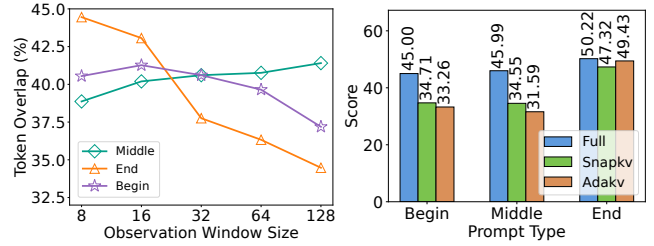
3.2.1 Motivational Observation 4: We reveal that relying solely on the last observation window of the input cannot reliably identify the important tokens from the input X_i for generating the output Y_i . Existing approaches, such as H2O [71], SnapKV [39], and AdaKV [18], propose selecting the top- B most important tokens $\hat{X}_i \subseteq X_i$ from the input X_i before generating the output tokens. Given the input X_i , we denote the last observation window of X_i with length n_s as $X_i^{obs} = X_i[n_i - n_s : n_i]$. Under the LLM model M_θ with n_h attention heads, these approaches select the top- B tokens $\hat{X}_i \subseteq X_i$ where $|\hat{X}_i| = B$ as follows:

$$\hat{X}_i = \arg \max_{\hat{X}_i \subseteq X_i} \sum_{j=1}^{n_h} \sum_{a \in \hat{X}_i} \sum_{b \in X_i^{obs}} A_i^k[a][b], \quad (4)$$

Then, given the output $Y_i = [x_{n_i+1}, x_{n_i+2}, \dots, x_{n_i+n_o}]$ corresponding to the input X_i , the ground-truth top- B important tokens $X_i^* \subseteq X_i$ can be obtained as follows:

$$\hat{X}_i^* = \arg \max_{\hat{X}_i \subseteq X_i} \sum_{j=1}^{n_h} \sum_{a \in \hat{X}_i} \sum_{b \in Y_i} A_i^k[a][b], \quad (5)$$

The overlap between \hat{X}_i and \hat{X}_i^* can be computed as $r_i = \frac{|\hat{X}_i \cap \hat{X}_i^*|}{B}$ and the average rate regarding the data \mathcal{D} is $\frac{\sum_{X_i \in \mathcal{D}} r_i}{|\mathcal{D}|}$. We set the budget $B = 0.1|X_i|$, corresponding to 10% of the tokens in each input X_i . We use Llama-3.1-8B-Instruct and construct the dataset from LongEval’s topic retrieval set [10], where each instance contains three topic contexts and an instruction (framed as a question) to summarize two of them. For each instance $X_i = (C_i, q_i)$, we create three variants by placing the instruction or question q_i at



(a) Important token overlapping. (b) Question in different position.

Figure 4: Question position matters. When user queries are not at the end of the input, both the identification of important input tokens and the task performance of KV compression methods decline, indicating their reliance on queries being at the end.

the beginning, middle, or end of the context C_i . As shown in Figure 4 (a), the average overlap of important tokens is highest when the question is at the end, but much lower when placed earlier, indicating that relying only on the last observation window misses relevant information unless the question appears last.

Also, as shown in Figure 4 (b), SnapKV [39] and AdaKV [18] perform similarly to the original LLM when the question is at the end of the input. However, their performance drops significantly when the question appears in the middle or at the beginning. It is because SnapKV [39] and AdaKV [18] rely on the last few tokens to select the most important tokens from the input. When the user questions are at the end of inputs, the last few tokens include the question itself, which helps identify tokens related to the question and generate high-quality outputs. In contrast, when the questions are placed in the beginning or middle, the last few tokens are unrelated to the questions and answers, making it difficult to identify the important tokens and leading to performance drop. This shows that current approaches depend heavily on the benchmark’s question placement, which does not reflect real-world input patterns. Consequently, they struggle to generalize to more realistic scenarios.

4 Multi-turn Long-Context Benchmarks

As discussed in Section 2.3, existing benchmarks mainly focus on single-turn tasks and place user queries at the end of the context, failing to reflect the complexity of real-world multi-turn dialogues. To address this, we propose a new multi-turn long-context benchmark that enables more comprehensive and realistic evaluation of LLMs in conversational scenarios, which is released in Huggingface.

4.1 The Design of Multi-turn LongBench

Each m -turn long-context data can be denoted as $\mathcal{D} = \{\mathcal{I}_i = [(C_{i,1}, q_{i,1}, a_{i,1}), (C_{i,2}, q_{i,2}, a_{i,2}), \dots, (C_{i,m}, q_{i,m}, a_{i,m})]\}_{i=1}^{|\mathcal{D}|}$, where $C_{i,j}$ is the context at the j -th turn of the instance \mathcal{I}_i , which can be empty, $q_{i,j}$ is the corresponding user question, and $a_{i,j}$ denotes the generated answer of the LLMs for $q_{i,j}$. We design diverse formats for each multi-turn long-context data instance as follows:

- **Diverse Query Positions:** For the j -th turn, given a context $C_{i,j} = \{C_{i,j}^1, C_{i,j}^2, \dots, C_{i,j}^p\}$ consisting of p distinct paragraphs

Table 3: Multi-turn dataset statistics.

Type	Dataset	D	#Turn	Avg Token	Metric
QA	NQA	500	3	30545.54	F1
	Qasper	500	3	5434.41	F1
	MFQA-en	500	3	7279.64	F1
	HotpotQA	500	3	13847.19	F1
	2WikiMQA	500	3	7471.16	F1
	Musique	500	3	16587.56	F1
Summary	MultiNews	500	2	2376.46	Rouge-L
	GovReport	500	2	9324.43	Rouge-L
	QMSum	500	2	12780.29	Rouge-L
Few-shot Learning	TREC	199	2	2293.99	Accuracy
	SAMSUM	199	2	3113.73	Accuracy

(e.g., segments), the query $q_{i,j}$ can be positioned at various locations within $C_{i,j}$. Specifically, it can appear at the beginning of $C_{i,j}$, at the end of $C_{i,j}$, or between two segments $C_{i,j}^k$ and $C_{i,j}^{k+1}$. Such a way addresses the limitation of existing methods, which only place the query at the end of the context. This placement may not accurately reflect real-world scenarios.

- **Diverse Query Relevance:** At the j -th turn, the answer $a_{i,j}$ to question $q_{i,j}$ is derived from the contexts $\{C_{i,j'}\}_{j'=1}^j$. In real user scenarios, the context sources for answering $q_{i,j}$ are diverse. Instead of restricting $q_{i,j}$ to rely solely on $C_{i,j}$, we design the answer $a_{i,j}$ to $q_{i,j}$ to come from a subset of contexts $C_{q_i} \subseteq \{C_{i,j'}\}_{j'=1}^j$, with the size of the subset varying as $|C_{q_i}| \in \{1, 2, \dots, j\}$.

4.2 Multi-turn LongBench Generation

Based on the above format, we design multi-turn long-context benchmarks across various categories to comprehensively evaluate the capabilities of LLMs. The detailed information for each dataset is presented in Table 3, and the specific methodology for constructing our proposed long-context benchmarks is outlined as follows:

- **Question Answering (QA).** These datasets are derived from the single-document QA and multi-document QA tasks in LongBench [5, 6], with each dataset comprising 500 instances. Each instance is structured into three turns. To construct these instances, we randomly select three question-answer pairs from a dataset in LongBench [5, 6] as the foundation for the three turns. The associated contexts are then systematically modified through splitting and recombination, with additional irrelevant contexts incorporated. This meticulous design ensures that each instance satisfies the requirements for diverse query positions and diverse query relevance, as outlined in Section 4.1.
- **Summarization.** These datasets are derived from the summarization tasks within LongBench [5, 6]. Each dataset comprises 500 instances, with each instance consisting of two turns. To enhance the diversity of the input, we randomly selected two instances from the original dataset and segmented their original contexts, subsequently recombining them into two turns. This process was carefully designed to ensure compliance with the diverse query relevance requirement outlined in Section 4.1. Finally, we annotated the source paragraphs for traceability and introduced additional noisy contexts to further enrich the complexity and challenge of the dataset.

Algorithm 1: LoopServe framework overview

Input: The m -turn input $\mathcal{I}_i = \{X_{i,j}\}_{j=1}^m$, LLM M_θ , threshold α , re-selection interval n_d , and budget B

Output: Answers $\{y_{i,j}\}_{j=1}^m$

- 1 $X_i \leftarrow \emptyset$
- 2 **for** $j = 1$ **to** m **do**
- 3 $X_i = X_i \cup y_{i,j-1} \cup X_{i,j}$, $\hat{X}_{i,j} = [y_{i,j-1}, X_{i,j}]$
 // Step 1: Parallel Prefilling Line Selection
- 4 **for** $k = 1$ **to** n_h **do**
- 5 $\hat{\mathcal{V}}_{i,j}^k, \hat{\mathcal{S}}_{i,j}^k = \text{PrefillingLineSelection}(M_\theta, X_i, \hat{X}_{i,j}, \alpha)$
- 6 // Step 2: KV Compression for Decoding
- 7 $\mathcal{L} = \{\hat{\mathcal{V}}_{i,j'}^k, \hat{\mathcal{S}}_{i,j'}^k\}_{j'=1, k=1}^{j, n_h}$
- 7 $y_{i,j} = \text{ProgressiveDecoding}(M_\theta, X_i, \mathcal{L}, n_d, B)$
- 8 **Return** Answers $\{y_{i,j}\}_{j=1}^m$.

- **Few-shot Learning.** These datasets are derived from the few-shot learning tasks in LongBench [5, 6]. To fulfill the requirements of diverse query positions and diverse query relevance as outlined in Section 4.1, we exclude instances containing fewer than four examples. For the remaining eligible instances, the examples are segmented and distributed across the first and second turns. The LLM is tasked with generating an initial response based on the examples provided in the first turn and subsequently refining its response in the second turn using the additional examples. Furthermore, the query is strategically positioned at the beginning, middle, and end of the examples to ensure diversity in query placement. To maintain the semantic integrity and structural completeness of the examples, regular expressions are employed for segmentation.

5 LoopLLM System

In this section, we first introduce an overview of the LoopServe framework and introduce its two key components: online pre-filling sparsification and progressive KV compression for decoding.

5.1 Framework Overview of LoopLLM System

The LoopServe framework addresses the inefficiencies of existing LLM inference systems in multi-turn dialogue scenarios, where traditional acceleration methods based on sparse attention or static KV compression use fixed patterns that cannot adapt to dynamic input and context changes. These methods often fail to maintain efficiency and conversational quality when handling long contexts or varied query positions. LoopServe overcomes these challenges with an adaptive dual-phase system that applies online attention sparsification in the prefilling phase and progressive KV compression in the decoding phase. It dynamically selects the most important parts of the attention matrix to reduce computation and iteratively compresses the KV cache by using generated output tokens to select relevant input tokens. For an m -turn input $\mathcal{I}_i = \{X_{i,j}\}_{j=1}^m$, where $X_{i,j}$ is the context or query in the j -th turn, LoopServe generates each answer $y_{i,j}$ using these two steps.

Step 1. Online Attention Head Sparsification in Prefilling.

To reduce the quadratic complexity of the attention matrix, we dynamically select the most important slash lines and vertical lines that capture the key attention weights. Specifically, in Algorithm 1 line 3-5, for each new input $X_{i,j}$ and the all inputs $X_i = \left(\cup_{j'=1}^{j-1} (X_{i,j'} \cup y_{i,j'})\right) \cup X_{i,j}$, we get $\hat{X}_{i,j} = [y_{i,j-1}, X_{i,j}]$ as the new appended input in the j turn. Then, for each k -th attention head, we first compute the attention matrix $A_i^k[\hat{X}_{i,j}] \in \mathbb{R}^{\hat{n}_{i,j} \times n_i}$, and then select the slash lines $\hat{S}_{i,j}^k$ and vertical lines $\hat{V}_{i,j}^k$ that collectively recover at least α of the total attention weight in $A_i^k[\hat{X}_{i,j}]$.

Step 2. Progressive KV Compression in Decoding. To address the high complexity of decoding, LoopServe progressively selects and stores only the most relevant tokens needed for generating subsequent outputs. Specifically, as described in Algorithm 1 (lines 7–14), after every re-selection interval n_d tokens, the framework uses the ProgressiveSelection function to compute a subset of input tokens $\hat{X}_i^k \subseteq X_i$ for each attention head k . these selected tokens \hat{X}_i^k are important for output generation. At each decoding step, LoopServe leverages the compressed KV cache $\{\hat{S}_{i,j'}^k, \hat{V}_{i,j'}^k\}_{j'=1, k}^{j, m_h}$ to generate the output sequence $y_{i,j}$.

5.2 Online Attention Sparsification in Prefilling

As discussed in Section 2.1, the prefilling phase incurs quadratic time complexity in the input length n because each attention matrix requires $O(n^2)$ computation. Sparsifying the attention matrix is therefore crucial for efficiency. However, as shown in **Key Point 1** in Section 3.1, attention matrix sparsity patterns are highly dynamic across inputs and even within the same attention head, making static or offline selection ineffective. To address this, we propose an online adaptive algorithm that, during prefilling, identifies and selects a subset of slash and vertical lines to recover at least an α fraction of the total attention weight for each head. This approach not only reduces computation but also enables efficient reuse of selected lines in subsequent dialogue turns, improving overall efficiency in multi-turn scenarios.

Definition 5.1 (Online Prefilling Sparsification Problem). Given the input sequence $X_i = \left(\cup_{j'=1}^{j-1} (X_{i,j'} \cup y_{i,j'})\right) \cup X_{i,j}$, where $y_{i,j'}$ is the answer for $X_{i,j'}$ and $X_{i,j}$ is the current turn’s input, consider the LLM model M_θ with n_h attention heads. We denote the concatenation of the previous answer $y_{i,j-1}$ and the current user input $X_{i,j}$ as $\hat{X}_{i,j} = [y_{i,j-1}, X_{i,j}]$, whose corresponding attention matrix requires sparsification. The k -th attention matrix between X_i and $\hat{X}_{i,j}$ is denoted as $A_i^k[\hat{X}_{i,j}] \in \mathbb{R}^{\hat{n}_{i,j} \times n_i}$. Let $S_{i,j}^k$ (resp., $V_{i,j}^k$) denote the set of all slash lines (resp., vertical lines) in $A_i^k[\hat{X}_{i,j}]$. The goal is to select a subset of slash lines $\hat{S}_{i,j}^k \subseteq S_{i,j}^k$ and a subset of vertical lines $\hat{V}_{i,j}^k \subseteq V_{i,j}^k$ such that together they recover at least an α fraction of the total attention weight in $A_i^k[\hat{X}_{i,j}]$, where $\alpha \in [0, 1]$.

$$\begin{aligned} \min \quad & \sum_{s \in \hat{S}_{i,j}^k} l_s + \sum_{v \in \hat{V}_{i,j}^k} l_v, \\ \text{s.t.} \quad & \sum_{(a,b) \in (\hat{S}_{i,j}^k \cup \hat{V}_{i,j}^k)} A_i^k[a][b] \geq \alpha \cdot \hat{n}_{i,j}, \end{aligned} \quad (6)$$

Algorithm 2: Adaptive Prefilling Sparsification Framework

Input: The input X_i and $\hat{X}_{i,j}$, k -th head of LLM M_θ , the parameter α

Output: The selected slash lines $\hat{S}_{i,j}^k$ and vertical lines $\hat{V}_{i,j}^k$

- 1 $\tilde{X}_{i,j} = \text{RandomSelect}(\hat{X}_{i,j})$
- 2 Compute Query $\tilde{Q}_{i,j}^k$ for $\tilde{X}_{i,j}$
- 3 Compute Key K_i^k for X_i
- 4 $A_i^k[\tilde{X}_{i,j}] = \text{Softmax}\left(\tilde{Q}_{i,j}^k (K_i^k)^\top / \sqrt{d_k}\right)$
- 5 $S_{i,j}^k = \text{SlashSum}(A_i^k[\tilde{X}_{i,j}])$, $V_{i,j}^k = \text{VerticalSum}(A_i^k[\tilde{X}_{i,j}])$
- 6 $S_{i,j}^k \leftarrow \text{Desc_Sort}(S_{i,j}^k)$, $V_{i,j}^k \leftarrow \text{Desc_Sort}(V_{i,j}^k)$
- 7 $\hat{S}_{i,j}^k \leftarrow \emptyset$, $\hat{V}_{i,j}^k \leftarrow \emptyset$
- 8 $ol_s = 0$, $ol_v = 0$, $sum = 0$
- 9 **while** $sum < \alpha \cdot \text{Sum}(A_i^k[\tilde{X}_{i,j}])$ **do**
- 10 $s = S_{i,j}^k[0]$, $v = V_{i,j}^k[0]$
- 11 $\Delta w_s = w_s - ol_s$, $\Delta w_v = w_v - ol_s$
- 12 **if** $\Delta w_s / (l_s - |\hat{V}_{i,j}^k|) \geq \Delta w_v / (l_v - |\hat{S}_{i,j}^k|)$ **then**
- 13 $\hat{S}_{i,j}^k = \hat{S}_{i,j}^k \cup \{s\}$, $ol_s = ol_s + w_s^{\max}$
- 14 $sum = sum + w_s - ol_v$
- 15 **else**
- 16 $\hat{V}_{i,j}^k = \hat{V}_{i,j}^k \cup \{v\}$, $ol_v = ol_v + w_v^{\max}$
- 17 $sum = sum + w_v - ol_s$
- 18 **Return** $\hat{S}_{i,j}^k$ and $\hat{V}_{i,j}^k$.

where $\hat{n}_{i,j}$ is the total attention weight in the matrix $A_i^k[\hat{X}_{i,j}]$, and l_s (resp., l_v) is the length of the slash line s (resp., vertical line v).

THEOREM 5.2. *The prefilling sparsification problem is NP-hard.*

PROOF. The Online Prefilling Sparsification Problem (OPSP) can be proven NP-hard via a reduction from the Set Cover Problem, a well-known NP-hard problem. The Set Cover Problem is defined as follows: given a universe $U = \{u_1, u_2, \dots, u_m\}$, a collection of subsets $\mathcal{P} = \{P_1, P_2, \dots, P_n\}$, the objective is to find a subset $\mathcal{P}^* \subseteq \mathcal{P}$ such that $\cup_{P_i \in \mathcal{P}^*} P_i = U$, and the total cost $\sum_{P_i \in \mathcal{P}^*} |P_i|$ is minimized. We map the elements of the Set Cover Problem to the OPSP as follows. Each element $u \in U$ corresponds to an entry in the attention matrix $A_i^k[\hat{X}_{i,j}]$ that needs to be covered. Each subset P_i in \mathcal{P} corresponds to a slash line s or a vertical line v in OPSP, which covers a subset of entries in the matrix. The cost of selecting subset P_i is mapped to the cost l_s (for slash lines s) or l_v (for vertical lines v) in OPSP. The Set Cover Problem’s requirement to cover all elements in U is equivalent to requiring α in OPSP. Therefore, if we can solve the OSOP optimally in polynomial time, we can solve the set cover problem in polynomial time. \square

Algorithm. Algorithm 2 takes as input the concatenated sequence $\hat{X}_{i,j} = [y_{i,j-1}, X_{i,j}]$, where $y_{i,j-1}$ is the previous answer and $X_{i,j}$ is the current user input. It also requires the k -th attention head of the LLM M_θ and a sparsity threshold parameter α . The output consists of selected slash lines $\hat{S}_{i,j}^k$ and selected vertical lines $\hat{V}_{i,j}^k$. The first step involves sampling a subset $\tilde{X}_{i,j}$ of the concatenated input $\hat{X}_{i,j}$, which reduces the computational cost of subsequent operations.

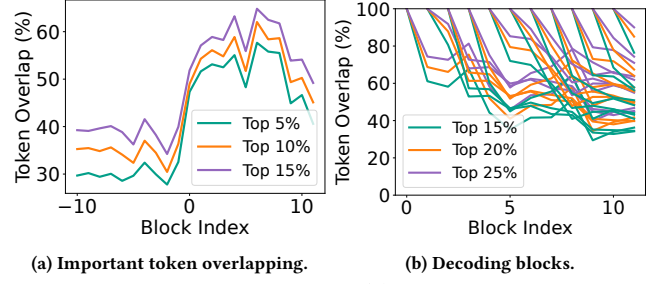
Next, Algorithm 2 computes the query matrix $\tilde{Q}_{i,j}^k$ for the sampled input $\tilde{X}_{i,j}$ and the key matrix K_i^k for the entire input X_i . Next, all slash lines $S_{i,j}^k$ and vertical lines $V_{i,j}^k$ are summarized based on $A_i^k[\tilde{X}_{i,j}]$ and sorted in descending order. Two empty sets, $\hat{S}_{i,j}^k$ and $\hat{V}_{i,j}^k$, are initialized to store the selected lines, and overlap weights ol_s and ol_v are set to zero. Then, Algorithm 2 iteratively selects lines until the total recovered attention weight sum meets or exceeds $\alpha \cdot \text{sum}(A_i^k[\tilde{X}_{i,j}])$. At each step, the top slash line $s \in S_{i,j}^k$ and the top vertical line $v \in V_{i,j}^k$ are compared based on their marginal contributions, $\Delta w_s = w_s - ol_v$ and $\Delta w_v = w_v - ol_s$. Particularly, since one slash line only has one overlap point with one vertical line, and thus $\Delta w_s = w_s - ol_v$. The line with the greater contribution is added to its respective set ($\hat{S}_{i,j}^k$ or $\hat{V}_{i,j}^k$), and the overlap weights and total recovered weight are updated accordingly. The loop ends once the recovery condition is satisfied, and the algorithm returns the sets $\hat{S}_{i,j}^k$ or $\hat{V}_{i,j}^k$.

Time Complexity Analysis. It is $O(n_i|\tilde{X}_{i,j}| + n_i \log n_i + n_i)$. Firstly, it takes $O(n_i|\tilde{X}_{i,j}|)$ to compute the partial attention matrix $A_i^k[\tilde{X}_{i,j}]$. Then, it takes $O(n_i|\tilde{X}_{i,j}|)$ to summarize the values for each slash line and vertical line, and takes $O(n_i \log n_i)$ for descending sorts. Finally, the greedy selection loop runs in $O(n_i)$.

5.3 Progressive KV Compression in Decoding

As discussed in Section 2.1.1, conventional decoding strategies often use fixed patterns or focus on the last few input tokens to select important information. However, as demonstrated in **Key Point 2** in Section 3.2, these methods are ineffective when user queries appear earlier in the input sequence. To address this, we propose a progressive KV compression strategy that dynamically selects important input tokens during decoding based on the most recently generated output tokens. This ensures that the selected tokens remain relevant throughout the generation process. Our analysis shows that using recent output tokens to guide selection leads to greater overlap with truly important input tokens, enhancing both efficiency and accuracy.

To verify this, we consider the LLM M_θ with n_h attention heads, the input sequence X_i , the generated output sequence Y_i , and a window size of n_w . Based on Equation (5), we compute the ground truth top- B important tokens $\hat{X}_i^* \subseteq X_i$ using the output Y_i . We then use an observation window extracted from either X_i or Y_i to select the top- B important tokens. Specifically, given the window size n_w , the $-\frac{|X_i|}{n_w}$ -th to -1 observation windows from the input X_i are defined as $X_i[n_i - m \cdot n_w : n_i - (m-1) \cdot n_w]$, $X_i[n_i - (m-1) \cdot n_w : n_i - (m-2) \cdot n_w]$, ..., $X_i[n_i - n_w : n_i]$, and the 0-th to $\frac{|Y_i|}{n_w}$ observation windows from the output Y_i are defined as $Y_i[0 : n_w]$, $Y_i[n_w : 2n_w]$, $Y_i[(m-1) \cdot n_w : m \cdot n_w]$. For each observation window X_i^{obs} from X_i or Y_i , we select the top- B tokens $\hat{X}_i \in X_i$ following Equation (4) and compute the overlap rate between \hat{X}_i and the ground truth \hat{X}_i^* as $\frac{|\hat{X}_i \cap \hat{X}_i^*|}{B}$. We use the same LongEval’s topic retrieval set [10] in Section 3 and Llama to conduct experiments, and set $B = \{5\%, 10\%, 15\%\} \cdot |X_i|$. As shown in Figure 5 (a), the overlap rate between the important tokens selected based on input block windows (block index < 0) is low. In contrast, the overlap rate



(a) Important token overlapping. (b) Decoding blocks.
Figure 5: Progressive decoding. (a) It shows that selecting important tokens from output windows yields higher overlap than from input windows, supporting progressive KV selection. (b) Also, the overlap between selected tokens in output blocks decreases with block distance, highlighting the need for progressive, output-driven cache updates.

Algorithm 3: Progressive Decoding

Input: Input \tilde{I}_i , LLM M_θ , all selected slash and vertical lines $\{\hat{V}_{i,j'}^k, \hat{S}_{i,j'}^k\}_{j'=1, k=1}^{n_h}$, re-selection interval n_d , and budget B

Output: Answer $y_{i,j}$

- 1 $n_o = 0, y_{i,j} = \emptyset$
 - 2 **while** LLM generation is not finished **do**
 - 3 **if** $n_o = 16$ or $(n_o - 16) \% n_d = 0$ **then**
 - 4 $X_i^{obs} = X_i[|X_i| - n_d : |X_i|]$
 - 5 **foreach** $k = 1$ to n_h **do** $\hat{X}_i^k \leftarrow$ Equation (7) ;
 - 6 $n_o = n_o + 1$
 - 7 $x_{n_i+n_o} = \text{Decoding}(M_\theta, \{\hat{X}_i^k\}_{k=1}^{n_h}, \{\hat{V}_{i,j'}^k, \hat{S}_{i,j'}^k\}_{j'=1, k=1}^{n_h})$
 - 8 $\hat{X}_i = \hat{X}_i \cup x_{n_i+n_o}, X_i = X_i \cup x_{n_i+n_o}$
 - 9 $y_{i,j} = y_{i,j} \cup x_{n_i+n_o}$
 - 10 **Return** Answer $y_{i,j}$
-

is significantly higher when important tokens are selected based on output block windows (block index ≥ 0). It demonstrates that leveraging output tokens to identify important input tokens is a more effective strategy for selecting relevant tokens.

We also observe that the overlap of important input tokens between output blocks decreases as the distance between the blocks increases. Specifically, given the output sequence Y_i , we divide it into n_b blocks, i.e., $Y_i = [Y_i^1, \dots, Y_i^{n_b}]$, where Y_i^j denotes the j -th output block with a size of $\frac{|Y_i|}{n_b}$. For each block Y_i^j , we compute the top- B important input tokens based on the attention weights as $\hat{X}_{i,Y_i^j} = \arg \max_{\hat{X}_i \subseteq X_i} \sum_{k=1}^{n_h} \sum_{a \in \hat{X}_i} \sum_{b \in Y_i^j} A_i^k[a][b]$. Next, we compare the overlap $|\hat{X}_{i,Y_i^j} \cap \hat{X}_{i,Y_i^{j'}}| / B$ of important input tokens between every pair of output blocks Y_i^j and $Y_i^{j'}$. As shown in Figure 5 (b), for each block Y_i^j , the overlap of important input tokens between Y_i^j and $Y_i^{j'}$ (where $j' > j$) gradually decreases as the block distance increases. Additionally, the overlap between Y_i^j and its immediate successor Y_i^{j+1} is higher compared to earlier blocks, such as Y_i^{j-2} . This indicates that tokens identified from Y_i^j are highly

relevant for the generation of Y_i^{j+1} . Therefore, when generating the output block Y_i^{j+1} , we leverage the preceding output block Y_i^j to dynamically identify the top- B important input tokens required for the generation of Y_i^{j+1} . This progressive approach ensures that the token selection remains relevant and efficient, reducing computational overhead while maintaining high accuracy.

Algorithm. Algorithm 3 firstly set the answer $y_{i,j}$ as empty and decoding step counter n_o to 0 (line 1). During the decoding loop, if the current step reaches either the empirically predefined decoding size 16 or a re-selection interval n_d (line 3), the algorithm extracts the most recent tokens from the input sequence X_i , i.e., $X_i^{obs} = X_i[|X_i| - n_d : |X_i|]$, and dynamically updates the compressed KV cache subset \hat{X}_i^k for each k -th attention head (line 4-5). Specifically, for each head, we select top- B tokens for each head as follows.

$$\hat{X}_i^k = \arg \max_{\hat{X}_i^k \subseteq X_i, |\hat{X}_i^k|=B} \sum_{a \in \hat{X}_i^k} \sum_{b \in X_i^{obs}} A_i^k[a][b], \quad (7)$$

The LLM generates the next token using the compressed KV cache and the updated input, which is appended to both the input and output sequences (line 6-9). This process iterates until the LLM completes generation, returning the final answer $y_{i,j}$.

6 EXPERIMENTS

We compare our LoopServe with six state-of-the-art KV cache algorithms on two representation LLM base models.

6.1 Experimental Settings

6.1.1 Datasets We designed the multi-turn long-context benchmark to rigorously evaluate LLMs in realistic conversational scenarios, addressing the limitations of single-turn benchmarks. Each instance comprises multiple rounds of context, queries, and answers, introducing diverse query positions and dependencies that reflect real-world conversational complexity. The benchmark covers three key categories: Question Answering, Summarization, and Few-shot Learning, using carefully curated datasets to ensure both diversity and complexity. Detailed dataset statistics are in Table 3.

6.1.2 Baselines In this study, we evaluate the performance of our proposed LoopServe algorithm against six competitive and state-of-the-art KV cache algorithms on Llama-3.1-8B-Instruct [21] and Qwen2.5-7B-Instruct [56], as well as the base model without any KV cache acceleration. The following KV cache methods are utilized for comparison:

- **SnapKV (Snap)** [39] optimizes KV caching through a snapshot mechanism, focusing on reducing redundant computations and enhancing memory utilization.
- **AdaKV (Ada)** [18] dynamically reallocates cache budgets across attention heads, shifting resources from heads with concentrated attention to those with dispersed patterns.
- **StreamingLLM (SLLM)** [62] maintains both attention sinks and a rolling window of recent tokens in its KV cache to enable stable infinite-length processing.
- **A-shape (A-S)** [62] sparses attention that resembles an A shape.
- **Tri-Shape (T-S)** [40] creates a triangular sparse attention pattern for pre-filling.

- **Minference (Minf)** [28] employs a minimal inference caching strategy to reduce computational overhead while maintaining effective KV cache management.

6.1.3 Evaluation Metrics. We adopt evaluation metrics for each dataset according to its task type. The metrics for each dataset are listed in Table 3. The details of the three metrics are as follows.

- **F1:** It is harmonic mean of precision and recall.
- **Accuracy:** Proportion of correct predictions over all predictions.
- **Rouge-L:** Measures the longest common subsequence (LCS) between generated and reference texts: Rouge-L = $\frac{LCS(C,R)}{|R|}$ where $LCS(C,R)$ is the length of the longest common subsequence between the candidate text C and the reference text R , and $|R|$ is the length of the reference text. This metric evaluates how well the generated text matches the reference sequence.

6.1.4 Hyperparameter and Hardware Setting All codes are executed on a Rocky Linux 8.10 machine with an 8-core Intel® Xeon® Gold 6542Y CPU, an NVIDIA H100 GPU with 80GB of memory, and 256GB of RAM. For baselines, we use their suggested default setting. For the main experiments in Section 6.2, for our LoopServe, we set $\alpha = 0.955$, and $n_d = 16$ as defaults, and we set the token selection budget $B = 1024$ for all baselines and LoopServe.

6.2 Main Experiments

6.2.1 Effectiveness Evaluation To evaluate the effectiveness of our proposed LoopServe and baselines, we conduct experiments on the proposed multi-turn long-context benchmark across three categories: Question Answering, Summarization, and Few-shot Learning. For each dataset, we compared LoopServe with six state-of-the-art KV cache acceleration baselines as well as the base LLMs, using the appropriate metrics (F1, Rouge-L, and Accuracy) for each task. As shown in Table 4, LoopServe achieves the best or comparable performance among KV compression baselines across a wide range of datasets and query positions. A key finding is that LoopServe maintains robust performance regardless of where the user query appears in the beginning, middle, or end of the input context. In contrast, existing baselines such as SnapKV and AdaKV exhibit a significant drop in performance when the query is not positioned at the end, highlighting their reliance on positional heuristics which do not generalize well to realistic dialogue settings. LoopServe’s adaptive approach, which dynamically selects relevant information both during prefilling and decoding, consistently leads to higher accuracy and quality, even as conversational context grows longer and more complex. Notably, these improvements are observed across both Llama-3.1 and Qwen2.5 models, indicating that LoopServe’s design generalizes well across different LLM architectures.

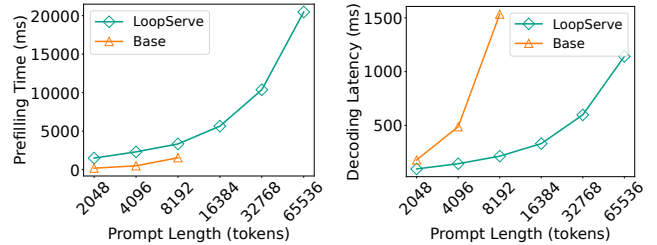
6.2.2 Efficiency Evaluation In addition to effectiveness, we also evaluate the efficiency of LoopServe in terms of prefilling time and decoding latency. As shown in Figure 6, LoopServe achieves substantial reductions in both prefilling time and inference time compared to the base LLM. The combination of efficient online sparsification and adaptive KV compression enables LoopServe to provide both high-quality outputs and rapid response times. Specifically, LoopServe’s online prefilling sparsification mechanism significantly reduces computational overhead by identifying and

Table 4: Effectiveness Evaluation. The bold number indicates the best performance among the baselines.

P	Data	Llama 3.1							Qwen2.5									
		Base	Snap	Ada	SLLM	A-S	T-S	Minf	Ours	Base	Snap	Ada	SLLM	A-S	T-S	Minf	Ours	
Begin	QA	MFQA-en	45.70	36.50	34.94	25.83	28.00	34.96	43.05	46.82	44.24	35.59	33.00	21.45	29.56	38.14	42.63	43.47
		2WikiMQA	31.68	29.31	28.73	22.05	19.42	24.20	28.57	35.11	37.86	34.54	33.83	23.19	22.11	32.90	35.33	37.52
		Musique	17.16	14.29	14.80	9.76	4.22	8.18	14.92	18.81	18.22	14.74	13.95	8.68	5.92	12.15	15.15	16.63
		HotpotQA	36.67	33.87	32.98	22.52	12.72	21.29	34.38	39.00	42.93	38.90	37.56	21.42	17.22	31.03	38.67	42.50
		NrtvQA	13.40	13.42	8.67	5.22	7.61	9.19	13.47	14.03	13.63	11.05	10.18	6.82	7.57	10.45	10.78	14.36
		Qasper	25.33	20.77	17.03	16.58	20.64	23.37	22.79	24.64	26.08	21.79	20.13	17.96	19.67	23.44	24.92	25.37
	SUM	MultiNews	20.08	19.20	18.03	19.30	20.10	20.15	20.25	20.14	18.39	15.87	14.52	17.29	18.29	18.30	18.30	20.14
		GovReport	25.25	18.36	16.53	17.98	24.16	24.13	24.55	24.90	20.93	16.80	15.86	15.90	22.28	21.90	20.86	23.60
		QMSum	20.53	17.49	17.56	14.66	17.77	18.92	20.15	20.65	19.97	17.54	17.39	14.66	18.45	19.12	19.61	19.66
	FS	TREC	46.99	46.74	45.23	46.23	41.21	46.99	45.48	47.99	65.08	64.07	63.32	62.65	60.30	56.28	64.07	65.33
		SAMSUM	17.32	16.75	16.48	12.95	17.39	17.35	17.46	18.12	16.19	13.97	13.15	11.22	15.32	15.92	15.96	17.15
	Middle	QA	MFQA-en	46.73	37.30	35.19	26.87	28.26	33.39	43.84	44.73	44.00	34.21	31.68	22.73	29.06	34.31	41.42
2WikiMQA			34.10	31.71	29.90	25.59	18.77	27.26	32.50	34.25	27.80	22.32	22.69	14.19	20.18	26.15	25.40	27.01
Musique			16.30	13.68	14.05	8.59	3.17	9.51	15.39	17.48	10.05	7.37	7.15	3.32	4.92	8.38	8.76	9.13
HotpotQA			40.63	37.48	36.30	27.30	12.36	25.25	36.81	41.25	29.43	25.24	24.56	12.25	12.96	22.00	26.43	29.05
NrtvQA			15.29	13.06	10.64	7.26	7.14	10.10	13.98	15.25	14.82	11.88	11.83	9.04	7.68	11.24	11.75	15.21
Qasper			30.79	26.80	22.07	21.40	24.90	28.86	28.47	31.12	28.74	23.57	21.77	20.75	24.73	27.84	28.72	29.27
SUM		MultiNews	20.59	19.78	18.12	19.91	20.49	20.52	20.79	20.66	18.37	15.54	14.28	17.53	18.09	18.26	18.19	18.44
		GovReport	24.08	18.39	15.92	18.09	23.50	24.01	23.74	22.88	20.54	16.24	15.25	15.99	21.00	21.55	20.70	20.68
		QMSum	20.51	17.90	17.84	15.08	17.62	17.93	20.20	20.41	20.04	17.79	17.29	15.06	18.57	18.67	19.46	19.81
FS		TREC	50.00	50.00	48.74	50.25	50.00	50.76	52.27	56.03	64.07	62.06	60.81	63.32	63.82	40.71	64.07	65.33
		SAMSUM	10.62	12.03	11.83	13.34	11.10	10.92	10.62	17.43	12.38	12.55	13.28	13.83	15.65	12.95	12.93	12.40
End		QA	MFQA-en	50.93	47.93	48.38	32.52	28.62	51.40	49.67	51.69	48.82	47.57	47.24	29.28	27.66	47.94	49.18
	2WikiMQA		42.43	42.34	41.96	37.20	25.19	39.54	41.75	44.05	42.70	42.25	41.24	32.89	26.50	37.54	41.34	42.24
	Musique		29.39	28.07	29.01	20.96	7.80	26.44	23.56	31.60	24.18	23.08	22.39	11.82	8.68	17.65	24.34	24.82
	HotpotQA		53.62	52.38	53.59	43.83	25.04	51.71	51.97	55.05	53.09	51.03	50.71	35.64	24.63	43.67	53.01	53.13
	NrtvQA		25.76	25.50	24.58	19.28	14.19	23.90	23.87	25.87	19.07	17.90	16.75	14.08	11.41	14.39	18.37	19.86
	Qasper		37.97	35.95	33.98	28.01	27.37	38.67	36.50	38.27	33.55	31.82	30.21	24.28	25.15	33.72	34.18	33.18
	SUM	MultiNews	20.59	20.03	18.87	19.97	20.16	20.40	20.49	20.45	18.31	16.61	15.32	17.74	17.99	18.01	18.36	18.40
		GovReport	23.90	20.10	18.54	18.04	23.17	23.35	23.92	24.27	21.21	18.06	17.09	16.95	21.53	21.82	21.28	21.10
		QMSum	22.69	22.21	22.12	19.67	18.59	22.28	22.27	22.82	21.17	20.15	20.03	18.13	18.07	20.33	21.04	20.95
	FS	TREC	59.05	58.54	58.54	58.54	52.51	59.55	59.05	60.31	68.34	66.08	66.59	67.84	63.82	67.59	68.85	68.34
		SAMSUM	18.78	23.88	20.63	19.84	18.45	17.75	17.62	23.53	39.46	39.58	38.77	38.71	39.13	39.20	39.57	39.85

selecting only the most critical components of the attention matrix. This targeted sparsification not only accelerates the prefilling stage but also reduces the memory footprint. During the decoding phase, LoopServe’s progressive KV compression dynamically maintains a compact and relevant KV cache, minimizing redundant computations and further improving inference speed.

6.2.3 *Ablation Study* To better understand the contribution of each component within LoopServe, we conducted ablation studies by evaluating two variants: LoopServe-D, which uses only progressive KV compression, and LoopServe-P, which applies only online prefilling sparsification. We conduct experiments on three datasets, i.e., MultifieldQA (MF), 2WikiMQA (2WM), and Qasper (Qsp), with both Llama and Qwen backbones. As shown in Figure 7, LoopServe delivers the highest and comparable performance, demonstrating that the integration of both online prefilling sparsification and progressive KV compression is essential for optimal results. The ablation study further reveals that these two components are complementary: while each addresses a different bottleneck in LLM inference,



(a) Prefilling time (time to first token). (b) Decoding latency (time between tokens). Lower is better.

Figure 6: Efficiency experiment. Base uses naive attention, and experiences OOM at length of 16384. We use Llama-3.1-8B-Instruct for experiment.

their combination ensures robust adaptation to diverse input patterns and maximizes both efficiency and accuracy. These findings are stable across all task types, datasets, and query positions, as well as for both tested LLM architectures.

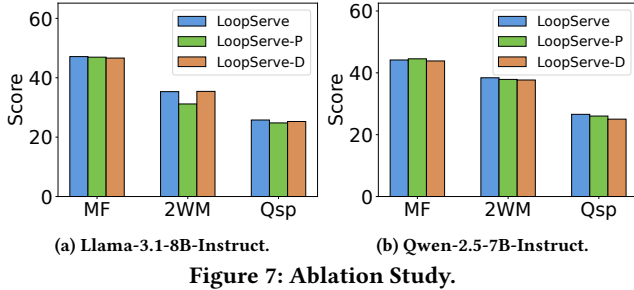


Figure 7: Ablation Study.

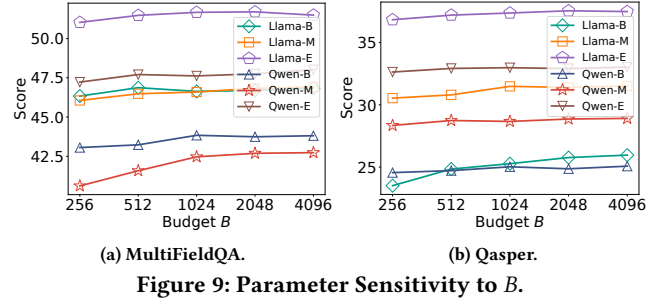


Figure 9: Parameter Sensitivity to B .

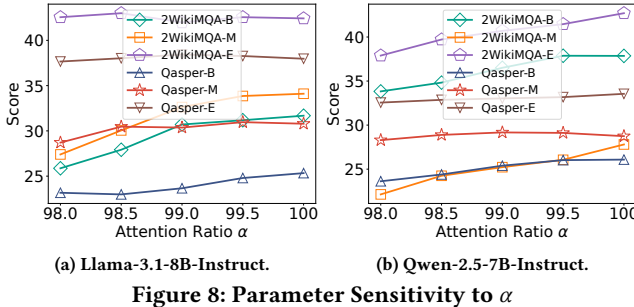


Figure 8: Parameter Sensitivity to α

6.3 Parameter Sensitivity

To further evaluate the robustness and adaptability of LoopServe, we conducted a parameter sensitivity analysis focusing on three key hyperparameters: the attention sparsity threshold α used in the online prefilling phase, and the token budget B and the decoding interval n_d in the progressive KV compression phase.

6.3.1 Threshold α in Equation (6). The parameter α determines how much total attention weight is preserved by the selected vertical and slash lines during online prefilling sparsification. Higher α retains more information but increases computation, while lower α improves efficiency at the risk of losing important context. Specifically, we conduct experiments on 2WikiMQA and Qasper data with Llama and Qwen backbones, containing questions at the beginning (-B), middle (-M), and end (-E) positions. We vary α within $\alpha \in \{0.980, 0.985, 0.990, 0.995, 1.00\}$. As shown in Figure 8, LoopServe achieves a favorable balance in the range of $\alpha = 0.99$ to $\alpha = 1.00$, where the accuracy remains high and the computational gains are significant. Notably, setting α too low can cause a drop in generation quality, while excessively high values diminish the efficiency benefits. These results indicate that LoopServe is not overly sensitive to the precise value of α within a reasonable range, and users can adjust this parameter to trade off between speed and output quality according to their application needs.

6.3.2 Budget B . The token selection budget B in LoopServe’s progressive KV compression impacts the balance between efficiency and output quality. Experiments conducted on MultiFieldQA and Qasper across three query positions (beginning, middle, and end). As shown in Table 9, increasing B generally improves performance, as retaining more tokens captures a larger portion of relevant context. However, beyond a threshold (e.g., 1024 tokens), the performance gains diminish, while computational and memory costs increase. Smaller budgets (e.g., 256 or 512) result in lower accuracy, particularly for queries in the beginning or middle of the input, as

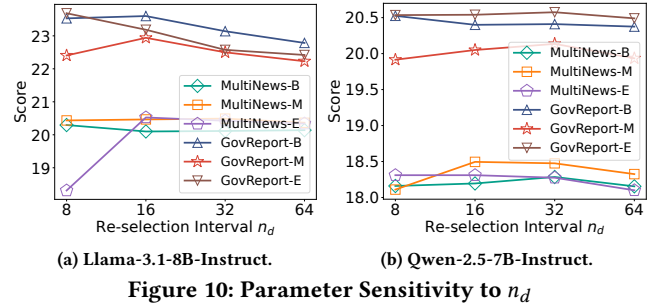


Figure 10: Parameter Sensitivity to n_d

key tokens may be excluded. In contrast, queries at the end are less sensitive to budget variations, as the most relevant tokens are naturally included in the cache. A budget of 1024 to 2048 tokens achieves the best balance, providing high performance across all query positions while maintaining computational efficiency.

6.3.3 The decoding interval n_d in Algorithm 3. The decoding interval n_d determines how frequently LoopServe re-selects important input tokens based on the most recent output during progressive KV compression. A smaller n_d allows the system to adapt more frequently to evolving output dependencies, which can further boost accuracy in challenging, dynamic dialogues. However, this comes with increased overhead due to more frequent KV cache updates. Specifically, we conduct experiments on MultiNews and GovReport data with Llama and Qwen backbones, containing questions at the beginning (-B), middle (-M), and end (-E) positions. As shown in Figure 10, our sensitivity analysis finds that moderate values of n_d (e.g., 16 or 32) provide the best balance: they preserve the majority of the efficiency gains while maintaining robust generation quality. Extremely large n_d values reduce the adaptivity of the KV cache and may result in decreased relevance of selected tokens, leading to lower performance on complex, multi-turn tasks.

7 Conclusion

In this paper, we propose LoopServe, an adaptive dual-phase LLM inference acceleration system designed for realistic multi-turn dialogues. By combining online attention sparsification and progressive KV compression, LoopServe addresses the limitations of static acceleration methods and adapts efficiently to dynamic conversational patterns. Our experiments on diverse, multi-turn benchmarks show that LoopServe significantly improves both inference speed and output quality compared to existing baselines, regardless of query position. This work provides a practical solution for efficient and effective LLM deployment in real-world dialogue scenarios.

References

- [1] Muhammad Adnan, Akhil Arunkumar, Gaurav Jain, Prashant J Nair, Ilya Solovychik, and Purushotham Kamath. 2024. Keyformer: Kv cache reduction through key tokens selection for efficient generative inference. *Proceedings of Machine Learning and Systems* 6 (2024), 114–127.
- [2] Chenxin An, Shansan Gong, Ming Zhong, Xingjian Zhao, Mukai Li, Jun Zhang, Lingpeng Kong, and Xipeng Qiu. 2023. L-Eval: Instituting Standardized Evaluation for Long Context Language Models. <https://doi.org/10.48550/ARXIV.2307.11088>
- [3] Yihao Ang, Yifan Bao, Qiang Huang, Anthony K. H. Tung, and Zhiyong Huang. 2024. TSGAssist: An Interactive Assistant Harnessing LLMs and RAG for Time Series Generation Recommendations and Benchmarking. *Proc. VLDB Endow.* 17, 12 (August 2024), 4309–4312. <https://www.vldb.org/pvldb/vol17/p4309-huang.pdf>
- [4] Simran Arora, Brandon Yang, Sabri Eyuboglu, Avani Narayan, Andrew Hojel, Immanuel Trummer, and Christopher Ré. 2023. Language models enable simple systems for generating structured views of heterogeneous data lakes. *arXiv preprint arXiv:2304.09433* (2023).
- [5] Yushi Bai, Xin Lv, Jiajie Zhang, Hongchang Lyu, Jiankai Tang, Zhidian Huang, Zhengxiao Du, Xiao Liu, Aohan Zeng, Lei Hou, Yuxiao Dong, Jie Tang, and Juanzi Li. 2024. LongBench: A Bilingual, Multitask Benchmark for Long Context Understanding. In *Proceedings of the 62nd Annual Meeting of the Association for Computational Linguistics (Volume 1: Long Papers)*. Association for Computational Linguistics, Bangkok, Thailand, 3119–3137. <https://doi.org/10.18653/v1/2024.acl-long.172>
- [6] Yushi Bai, Shangqing Tu, Jiajie Zhang, Hao Peng, Xiaozhi Wang, Xin Lv, Shulin Cao, Jiazheng Xu, Lei Hou, Yuxiao Dong, Jie Tang, and Juanzi Li. 2024. LongBench v2: Towards Deeper Understanding and Reasoning on Realistic Long-context Multitasks. *arXiv preprint arXiv:2412.15204* (2024).
- [7] Tom Brown, Benjamin Mann, Nick Ryder, Melanie Subbiah, Jared D Kaplan, Prafulla Dhariwal, Arvind Neelakantan, Pranav Shyam, Girish Sastry, Amanda Askell, Sandhini Agarwal, Ariel Herbert-Voss, Gretchen Krueger, Tom Henighan, Rewon Child, Aditya Ramesh, Daniel Ziegler, Jeffrey Wu, Clemens Winter, Chris Hesse, Mark Chen, Eric Sigler, Mateusz Litwin, Scott Gray, Benjamin Chess, Jack Clark, Christopher Berner, Sam McCandlish, Alec Radford, Ilya Sutskever, and Dario Amodei. 2020. Language Models are Few-Shot Learners. In *Advances in Neural Information Processing Systems*, H. Larochelle, M. Ranzato, R. Hadsell, M.F. Balcan, and H. Lin (Eds.), Vol. 33. Curran Associates, Inc., 1877–1901. https://proceedings.neurips.cc/paper_files/paper/2020/file/1457c0d6bfc4967418bfb8ac142f64a-Paper.pdf
- [8] Kaiwen Chen and Nick Koudas. 2024. Unstructured Data Fusion for Schema and Data Extraction. *Proc. ACM Manag. Data* 2, 3, Article 181 (May 2024), 26 pages. <https://doi.org/10.1145/3654984>
- [9] Sibe Chen, Ju Fan, Bin Wu, Nan Tang, Chao Deng, Pengyi Wang, Ye Li, Jian Tan, Feifei Li, Jingren Zhou, et al. 2025. Automatic Database Configuration Debugging using Retrieval-Augmented Language Models. *Proceedings of the ACM on Management of Data* 3, 1 (2025), 1–27.
- [10] Anze Xie Ying Sheng Lianmin Zheng Joseph E. Gonzalez Ion Stoica Xuezhe Ma Dacheng Li*, Rulin Shao* and Hao Zhang. 2023. How Long Can Open-Source LLMs Truly Promise on Context Length? <https://lmsys.org/blog/2023-06-29-longchat>
- [11] Arash Dargahi Nobari and Davood Rafiei. 2024. Dtt: An example-driven tabular transformer for joinability by leveraging large language models. *Proceedings of the ACM on Management of Data* 2, 1 (2024), 1–24.
- [12] DeepSeek-AI. 2024. DeepSeek-V3 Technical Report. *arXiv:2412.19437* [cs.CL] <https://arxiv.org/abs/2412.19437>
- [13] DeepSeek-AI. 2025. DeepSeek-R1: Incentivizing Reasoning Capability in LLMs via Reinforcement Learning. *arXiv:2501.12948* [cs.CL] <https://arxiv.org/abs/2501.12948>
- [14] Cheng Deng, Luoyang Sun, Jiwen Jiang, Yongcheng Zeng, Xinjian Wu, Wenxin Zhao, Qingfa Xiao, Jiachuan Wang, Haoyang Li, Lei Chen, et al. 2025. PLM: Efficient Peripheral Language Models Hardware-Co-Designed for Ubiquitous Computing. *arXiv preprint arXiv:2503.12167* (2025).
- [15] Darren Edge, Ha Trinh, Newman Cheng, Joshua Bradley, Alex Chao, Apurva Mody, Steven Truitt, Dasha Metropolitan, Robert Osazuwa Ness, and Jonathan Larson. 2024. From local to global: A graph rag approach to query-focused summarization. *arXiv preprint arXiv:2404.16130* (2024).
- [16] Mohamed Y. Eltabakh, Zan Ahmad Naeem, Mohammad Shahmeer Ahmad, Mourad Ouzzani, and Nan Tang. 2024. RetClean: Retrieval-Based Tabular Data Cleaning Using LLMs and Data Lakes. *Proc. VLDB Endow.* 17, 12 (August 2024), 4421–4424. <https://www.vldb.org/pvldb/vol17/p4421-eltabakh.pdf>
- [17] Ju Fan, Zihui Gu, Songyue Zhang, Yuxin Zhang, Zui Chen, Lei Cao, Guoliang Li, Samuel Madden, Xiaoyong Du, and Nan Tang. 2024. Combining Small Language Models and Large Language Models for Zero-Shot NL2SQL. *Proc. VLDB Endow.* 17, 11 (July 2024), 2750–2763. <http://dblp.uni-trier.de/db/journals/pvldb/pvldb17.html#FanGZZCCLMDT24>
- [18] Yuan Feng, Junlin Lv, Yukun Cao, Xike Xie, and S Kevin Zhou. 2024. Ada-kv: Optimizing kv cache eviction by adaptive budget allocation for efficient llm inference. *arXiv preprint arXiv:2407.11550* (2024).
- [19] Benjamin Feuer, Yurong Liu, Chinnmay Hegde, and Juliana Freire. 2024. ArcheType: A Novel Framework for Open-Source Column Type Annotation using Large Language Models. *Proc. VLDB Endow.* 17, 9 (May 2024), 2279–2292. <https://www.vldb.org/pvldb/vol17/p2279-freire.pdf>
- [20] Suyu Ge, Yunan Zhang, Liyuan Liu, Minjia Zhang, Jiawei Han, and Jianfeng Gao. 2024. Model Tells You What to Discard: Adaptive KV Cache Compression for LLMs. In *The Twelfth International Conference on Learning Representations, ICLR 2024, Vienna, Austria, May 7–11, 2024*. OpenReview.net.
- [21] Aaron Grattafiori, Abhimanyu Dubey, and others]. 2024. The Llama 3 Herd of Models. *arXiv:2407.21783* [cs.AI] <https://arxiv.org/abs/2407.21783>
- [22] Muhammad Usman Hadi, Rizwan Qureshi, Abbas Shah, Muhammad Irfan, Anas Zafar, Muhammad Bilal Shaikh, Naveed Akhtar, Jia Wu, Seyedali Mirjalili, et al. 2023. A survey on large language models: Applications, challenges, limitations, and practical usage. *Authorea Preprints* 3 (2023).
- [23] Alon Y. Halevy, Yuliang Li, and Wang-Chiew Tan. 2024. Personal Manifold: Management of Personal Data in the Age of Large Language Models. In *ICDE*. 5523–5529. <https://doi.org/10.1109/ICDE60146.2024.00440>
- [24] Cheng-Ping Hsieh, Simeng Sun, Samuel Kriman, Shantanu Acharya, Dima Rekeshe, Fei Jia, Yang Zhang, and Boris Ginsburg. 2024. RULER: What’s the Real Context Size of Your Long-Context Language Models? *arXiv preprint arXiv:2404.06654* (2024).
- [25] Chuxuan Hu, Austin Peters, and Daniel Kang. 2024. LEAP: LLM-Powered End-to-End Automatic Library for Processing Social Science Queries on Unstructured Data. *Proc. VLDB Endow.* 18, 2 (Oct. 2024), 253–264. <https://doi.org/10.14778/3705829.3705843>
- [26] Yuncheng Huang, Qianyu He, Jiaqing Liang, Sihang Jiang, Yanghua Xiao, and Yunwen Chen. 2024. Enhancing Quantitative Reasoning Skills of Large Language Models through Dimension Perception. In *2024 IEEE 40th International Conference on Data Engineering (ICDE)*. IEEE Computer Society, Los Alamitos, CA, USA, 789–802. <https://doi.org/10.1109/ICDE60146.2024.00066>
- [27] Nan Huo, Reynold Cheng, Ben Kao, Wentao Ning, Nur Al Hasan Halder, Xiaodong Li, Jinyang Li, Mohammad Matin Najafi, Tian Li, and Ge Qu. 2024. ZeroEA: A Zero-Training Entity Alignment Framework via Pre-Trained Language Model. *Proc. VLDB Endow.* 17, 7 (March 2024), 1765–1774. <http://dblp.uni-trier.de/db/journals/pvldb/pvldb17.html#HuoCKNHLNLQ24>
- [28] Huiqiang Jiang, Yucheng Li, Chengruidong Zhang, Qianhui Wu, Xufang Luo, Surin Ahn, Zhenhua Han, Amir H Abdi, Dongsheng Li, Chin-Yew Lin, et al. 2024. Minference 1.0: Accelerating pre-filling for long-context llms via dynamic sparse attention. *arXiv preprint arXiv:2407.02490* (2024).
- [29] Huiqiang Jiang, Qianhui Wu, Chin-Yew Lin, Yuqing Yang, and Lili Qiu. 2023. LLMingua: Compressing Prompts for Accelerated Inference of Large Language Models. In *Proceedings of the 2023 Conference on Empirical Methods in Natural Language Processing*. 13358–13376.
- [30] Wenqi Jiang, Marco Zeller, Roger Waleffe, Torsten Hoefler, and Gustavo Alonso. 2024. Chameleon: a Heterogeneous and Disaggregated Accelerator System for Retrieval-Augmented Language Models. *Proc. VLDB Endow.* 18, 1 (2024), 42–52. <https://www.vldb.org/pvldb/vol18/p42-jiang.pdf>
- [31] Yekyung Kim, Jenna Russell, Marzena Karpinska, and Mohit Iyyer. 2025. One ruler to measure them all: Benchmarking multilingual long-context language models. *arXiv:2503.01996* [cs.CL] <https://arxiv.org/abs/2503.01996>
- [32] Xunhao Lai, Jianqiao Lu, Yao Luo, Yiyuan Ma, and Xun Zhou. 2025. FlexPrefix: A Context-Aware Sparse Attention Mechanism for Efficient Long-Sequence Inference. In *The Thirteenth International Conference on Learning Representations*. <https://openreview.net/forum?id=OfjllbelrT>
- [33] Duy Le, Kris Zhao, Mengying Wang, and Yinghui Wu. 2024. GraphLingo: Domain Knowledge Exploration by Synchronizing Knowledge Graphs and Large Language Models. In *2024 IEEE 40th International Conference on Data Engineering (ICDE)*. IEEE, 5477–5480.
- [34] Boyan Li, Yuyu Luo, Chengliang Chai, Guoliang Li, and Nan Tang. 2024. The Dawn of Natural Language to SQL: Are We Fully Ready? *Proc. VLDB Endow.* 17, 11 (July 2024), 3318–3331. <http://dblp.uni-trier.de/db/journals/pvldb/pvldb17.html#LiLCLT24>
- [35] Guoliang Li, Xuanhe Zhou, and Xinyang Zhao. 2024. LLM for Data Management. *Proc. VLDB Endow.* 17, 12 (Aug. 2024), 4213–4216. <https://doi.org/10.14778/3685800.3685838>
- [36] Haoyang Li, Xuejia Chen, Zhanchao XU, Darian Li, Nicole Hu, Fei Teng, Yiming Li, Luyu Qiu, Chen Jason Zhang, Qing Li, and Lei Chen. 2025. Exposing Numeracy Gaps: A Benchmark to Evaluate Fundamental Numerical Abilities in Large Language Models. *arXiv:2502.11075* [cs.CL] <https://arxiv.org/abs/2502.11075>
- [37] Haoyang Li, Yiming Li, Anxin Tian, Tianhao Tang, Zhanchao Xu, Xuejia Chen, Nicole Hu, Wei Dong, Qing Li, and Lei Chen. 2024. A Survey on Large Language Model Acceleration based on KV Cache Management. *CoRR* abs/2412.19442 (2024). <http://dblp.uni-trier.de/db/journals/corr/corr2412.html#abs-2412-19442>
- [38] Qinbin Li, Junyuan Hong, Chulin Xie, Jeffrey Tan, Rachel Xin, Junyi Hou, Xavier Yin, Zhun Wang, Dan Hendrycks, Zhangyang Wang, Bo Li, Bingsheng He, and

- Dawn Song. 2024. LLM-PBE: Assessing Data Privacy in Large Language Models. *Proc. VLDB Endow.* 17, 11 (July 2024), 3201–3214. <https://www.vldb.org/pvldb/vol17/p3201-li.pdf>
- [39] Yuhong Li, Yingbing Huang, Bowen Yang, Bharat Venkitesh, Acyr Locatelli, Hanchen Ye, Tianle Cai, Patrick Lewis, and Deming Chen. 2024. Snapkv: Llm knows what you are looking for before generation. *Advances in Neural Information Processing Systems* 37 (2024), 22947–22970.
- [40] YUCHENG LI, Huiqiang Jiang, Qianhui Wu, Xufang Luo, Surin Ahn, Chengruidong Zhang, Amir H. Abdi, Dongsheng Li, Jianfeng Gao, Yuqing Yang, and Lili Qiu. 2025. SCBench: A KV Cache-Centric Analysis of Long-Context Methods. In *The Thirteenth International Conference on Learning Representations*. <https://openreview.net/forum?id=gkUyY1W9>
- [41] Yuze Lou, Chuan Lei, Xiao Qin, Zichen Wang, Christos Faloutsos, Rishita Anubhai, and Huzefa Rangwala. 2024. DATAFORE: Can a Large Language Model Find All Lost Scrolls in a Data Repository?. In *2024 IEEE 40th International Conference on Data Engineering (ICDE)*, 5170–5176. <https://doi.org/10.1109/ICDE60146.2024.00388>
- [42] Kyle Luoma and Arun Kumar. 2025. SNAILS: Schema Naming Assessments for Improved LLM-Based SQL Inference. *Proc. ACM Manag. Data* 3, 1 (February 2025), 77:1–77:26. <http://dblp.uni-trier.de/db/journals/pacmmod/pacmmod3.html#LuomaK25>
- [43] Junlin Lv, Yuan Feng, Xike Xie, Xin Jia, Qirong Peng, and Guiming Xie. 2024. CritiPrefill: A Segment-wise Criticality-based Approach for Prefilling Acceleration in LLMs. *arXiv preprint arXiv:2409.12490* (2024).
- [44] Kabir Nagrecha and Arun Kumar. 2023. Saturn: An Optimized Data System for Multi-Large-Model Deep Learning Workloads. *Proc. VLDB Endow.* 17, 4 (2023), 712–725. <https://doi.org/10.14778/3636218.3636227>
- [45] Wei Ni, Xiaoye Miao, Xiangyu Zhao, Yangyang Wu, Shuwei Liang, and Jianwei Yin. 2024. Automatic Data Repair: Are We Ready to Deploy? *Proc. VLDB Endow.* 17, 10 (June 2024), 2617–2630. <https://doi.org/10.14778/3675034.3675051>
- [46] Reham Omar, Omij Mangukiya, and Essam Mansour. 2025. Dialogue Benchmark Generation from Knowledge Graphs with Cost-Effective Retrieval-Augmented LLMs. *Proceedings of the ACM on Management of Data* 3, 1 (2025), 1–26.
- [47] Zhuoshi Pan, Qianhui Wu, Huiqiang Jiang, Menglin Xia, Xufang Luo, Jue Zhang, Qingwei Lin, Victor Rühle, Yuqing Yang, Chin-Yew Lin, et al. 2024. LlmLingua-2: Data distillation for efficient and faithful task-agnostic prompt compression. *arXiv preprint arXiv:2403.12968* (2024).
- [48] Yanzhao Qin, Tao Zhang, Tao Zhang, Yanjun Shen, Wenjing Lou, Haoze Sun, Yan Zhang, Yujing Qiao, Weipeng Chen, Zenan Zhou, Wentao Zhang, and Bin Cui. 2024. SysBench: Can Large Language Models Follow System Messages? *arXiv:2408.10943 [cs.CL]* <https://arxiv.org/abs/2408.10943>
- [49] Alec Radford, Karthik Narasimhan, Tim Salimans, Ilya Sutskever, et al. 2018. Improving language understanding by generative pre-training. (2018).
- [50] Alec Radford, Jeffrey Wu, Rewon Child, David Luan, Dario Amodei, Ilya Sutskever, et al. 2019. Language models are unsupervised multitask learners. *OpenAI blog* 1, 8 (2019), 9.
- [51] Tonghui Ren, Yuankai Fan, Zhenying He, Ren Huang, Jiaqi Dai, Can Huang, Yinan Jing, Kai Zhang, Yifan Yang, and X. Sean Wang. 2024. PURPLE: Making a Large Language Model a Better SQL Writer.. In *ICDE. IEEE*, 15–28. <http://dblp.uni-trier.de/db/conf/icde/icde2024.html#RenFHHHJZYW24>
- [52] Shreya Shankar, Haotian Li, Parth Asawa, Madelon Hulsebos, Yiming Lin, J. D. Zamfirescu-Pereira, Harrison Chase, Will Fu-Hinthorn, Aditya G. Parameswaran, and Eugene Wu. 2024. spade: Synthesizing Data Quality Assertions for Large Language Model Pipelines. *Proc. VLDB Endow.* 17, 12 (Aug. 2024), 4173–4186. <https://doi.org/10.14778/3685800.3685835>
- [53] Mukul Singh, José Cambronero, Sumit Gulwani, Vu Le, Carina Negreanu, Elnaz Nouri, Mohammad Raza, and Gust Verbruggen. 2023. FormATS: Abstraction and Examples for Conditional Table Formatting with Natural Language. *Proc. VLDB Endow.* 17, 3 (Nov. 2023), 497–510. <https://doi.org/10.14778/3632093.3632111>
- [54] Yushi Sun, Hao Xin, Kai Sun, Yifan Ethan Xu, Xiao Yang, Xin Luna Dong, Nan Tang, and Lei Chen. 2024. Are Large Language Models a Good Replacement of Taxonomies? *Proc. VLDB Endow.* 17, 11 (July 2024), 2919–2932. <https://doi.org/10.14778/3681954.3681973>
- [55] Xiu Tang, Wenhao Liu, Sai Wu, Chang Yao, Gongsheng Yuan, Shanshan Ying, and Gang Chen. 2024. QueryArtisan: Generating Data Manipulation Codes for Ad-hoc Analysis in Data Lakes. *Proc. VLDB Endow.* 18, 2 (2024), 108–116. <https://www.vldb.org/pvldb/vol18/p108-yao.pdf>
- [56] Qwen Team. 2024. Qwen2.5: A Party of Foundation Models. <https://qwenlm.github.io/blog/qwen2.5/>
- [57] Hugo Touvron, Thibaut Lavril, Gautier Izacard, Xavier Martinet, Marie-Anne Lachaux, Timothée Lacroix, Baptiste Rozière, Naman Goyal, Eric Hambro, Faisal Azhar, et al. 2023. Llama: Open and efficient foundation language models. *arXiv preprint arXiv:2302.13971* (2023).
- [58] Alexander van Renen, Mihail Stoian, and Andreas Kipf. 2024. DataLoom: Simplifying Data Loading with LLMs. *Proc. VLDB Endow.* 17, 12 (August 2024), 4449–4452. <http://dblp.uni-trier.de/db/journals/pvldb/pvldb17.html#RenenSK24>
- [59] A Vaswani. 2017. Attention is all you need. *Advances in Neural Information Processing Systems* (2017).
- [60] Yubo Wang, Haoyang Li, Fei Teng, and Lei Chen. 2025. Graph-based Retrieval Augmented Generation for Dynamic Few-shot Text Classification. *arXiv preprint arXiv:2501.02844* (2025).
- [61] Yang Wu, Yao Wan, Hongyu Zhang, Yulei Sui, Wucui Wei, Wei Zhao, Guandong Xu, and Hai Jin. 2024. Automated data visualization from natural language via large language models: An exploratory study. *Proceedings of the ACM on Management of Data* 2, 3 (2024), 1–28.
- [62] Guangxuan Xiao, Yuandong Tian, Beidi Chen, Song Han, and Mike Lewis. 2024. Efficient Streaming Language Models with Attention Sinks. In *The Twelfth International Conference on Learning Representations*. <https://openreview.net/forum?id=NG7sS51zVF>
- [63] Siqiao Xue, Danrui Qi, Caigao Jiang, Fangyin Cheng, Keting Chen, Zhiping Zhang, Hongyang Zhang, Ganglin Wei, Wang Zhao, Fan Zhou, Hong Yi, Shaodong Liu, Hongjun Yang, and Faqiang Chen. 2024. Demonstration of DB-GPT: Next Generation Data Interaction System Empowered by Large Language Models. *Proc. VLDB Endow.* 17, 12 (August 2024), 4365–4368. <https://www.vldb.org/pvldb/vol17/p4365-chen.pdf>
- [64] Mengyi Yan, Yaoshu Wang, Yue Wang, Xiaoye Miao, and Jianxin Li. 2024. GIDCL: A Graph-Enhanced Interpretable Data Cleaning Framework with Large Language Models. *Proc. ACM Manag. Data* 2, 6 (2024), 236:1–236:29. <https://doi.org/10.1145/3698811>
- [65] Feng Yao, Qian Tao, Wenyuan Yu, Yanfeng Zhang, Shufeng Gong, Qiange Wang, Ge Yu, and Jingren Zhou. 2023. RAGGraph: A Region-Aware Framework for Geo-Distributed Graph Processing. *Proc. VLDB Endow.* 17, 3 (November 2023), 264–277. <http://dblp.uni-trier.de/db/journals/pvldb/pvldb17.html#YaoTYZGWYZ23>
- [66] Chanwoong Yoon, Taewho Lee, Hyeon Hwang, Minbyul Jeong, and Jaewoo Kang. 2024. Compact: Compressing retrieved documents actively for question answering. *arXiv preprint arXiv:2407.09014* (2024).
- [67] Runjie Yu, Weizhou Huang, Shuhan Bai, Jian Zhou, and Fei Wu. 2025. AquaPipe: A Quality-Aware Pipeline for Knowledge Retrieval and Large Language Models. *Proc. ACM Manag. Data* 3, 1 (2025), 11:1–11:26. <https://doi.org/10.1145/3709661>
- [68] Hailin Zhang, Xiaodong Ji, Yilin Chen, Fangcheng Fu, Xupeng Miao, Xiaonan Nie, Weipeng Chen, and Bin Cui. 2025. PQCACHE: Product Quantization-based KVCache for Long Context LLM Inference. *arXiv:2407.12820 [cs.CL]* <https://arxiv.org/abs/2407.12820>
- [69] Meihui Zhang, Zhaoxuan Ji, Zhaojing Luo, Yuncheng Wu, and Chengliang Chai. 2024. Applications and challenges for large language models: From data management perspective. In *2024 IEEE 40th International Conference on Data Engineering (ICDE)*. IEEE, 5530–5541.
- [70] Yi Zhang, Jan Deriu, George Katsogiannis-Meimarakis, Catherine Kosten, Georgia Koutrika, and Kurt Stockinger. 2023. ScienceBenchmark: A Complex Real-World Benchmark for Evaluating Natural Language to SQL Systems. *Proc. VLDB Endow.* 17, 4 (2023), 685–698. <https://doi.org/10.14778/3636218.3636225>
- [71] Zhenyu Zhang, Ying Sheng, Tianyi Zhou, Tianlong Chen, Lianmin Zheng, Ruisi Cai, Zhao Song, Yuandong Tian, Christopher Ré, Clark Barrett, et al. 2023. H2o: Heavy-hitter oracle for efficient generative inference of large language models. *Advances in Neural Information Processing Systems* 36 (2023), 34661–34710.
- [72] Xinyang Zhao, Xuanhe Zhou, and Guoliang Li. 2024. Chat2data: An interactive data analysis system with rag, vector databases and llms. *Proceedings of the VLDB Endowment* 17, 12 (2024), 4481–4484.
- [73] Bowen Zheng, Yupeng Hou, Hongyu Lu, Yu Chen, Wayne Xin Zhao, Ming Chen, and Ji-Rong Wen. 2024. Adapting Large Language Models by Integrating Collaborative Semantics for Recommendation.. In *ICDE. IEEE*, 1435–1448. <http://dblp.uni-trier.de/db/conf/icde/icde2024.html#ZhengHLZCZW24>
- [74] Xuanhe Zhou, Zhaoyan Sun, and Guoliang Li. 2024. Db-gpt: Large language model meets database. *Data Science and Engineering* 9, 1 (2024), 102–111.
- [75] Jun-Peng Zhu, Peng Cai, Boyan Niu, Zheming Ni, Kai Xu, Jiajun Huang, Jianwei Wan, Shengbo Ma, Bing Wang, Donghui Zhang, Liu Tang, and Qi Liu. 2024. Chat2Query: A Zero-Shot Automatic Exploratory Data Analysis System with Large Language Models.. In *ICDE. IEEE*, 5429–5432. <http://dblp.uni-trier.de/db/conf/icde/icde2024.html#ZhuCNNXHWZWZTL24>
- [76] Jun-Peng Zhu, Peng Cai, Kai Xu, Li Li, Yishen Sun, Shuai Zhou, Haihuang Su, Liu Tang, and Qi Liu. 2024. AutoTQA: Towards Autonomous Tabular Question Answering through Multi-Agent Large Language Models. *Proc. VLDB Endow.* 17 (2024), 3920–3933. <https://api.semanticscholar.org/CorpusID:272727897>
- [77] Zhen Zhu, Yibo Wang, Shouqing Yang, Lin Long, Runze Wu, Xiu Tang, Junbo Zhao, and Haobo Wang. 2024. CORAL: Collaborative Automatic Labeling System based on Large Language Models. *Proc. VLDB Endow.* 17, 12 (August 2024), 4401–4404. <https://www.vldb.org/pvldb/vol17/p4401-zhu.pdf>